ABSTRACT

Title of Document: TinyTerp: A FULLY AUTONOMOUS MOBILE SMART CENTI-ROBOT

George Mikeal Gateau III
Master of Science, 2011

Directed By: Professor Sarah Bergbreiter
Department of Mechanical Engineering and
The Institute for Systems Research

A fully autonomous modular 8 cm^3 robot is presented using commercially available off-the-shelf (COTS) components. The robot introduced is called Tiny Terrestrial Robotic Platform (TinyTeRP) which provides an inexpensive, easily assembled, small robotic platform for researchers to study swarm behavior. TinyTeRP can be assembled in 30 minutes and costs $51.50. TinyTeRP is fully autonomous, with approximately 10 minutes of run time, and the ability to travel over 20 cm/s with DC motors and wheels. Communication to other TinyTeRP robots and stationary sensors is performed using a 2.4 GHz IEEE 802.15.4 radio. TinyTeRP has the ability to interface with additional sensors modules and locomotion actuators, including a wheeled locomotion and inertial measurement unit (IMU) module. An additional legged platform module that uses thermally actuated polymer legs with a silver composite acrylic is discussed. Finally, TinyTeRP demonstrates the use of two control algorithms to interact with a fixed beacon using received signal strength indicator (RSSI).

TinyTerp: FULLY AUTONOMOUS MODULAR MICRO-ROBOT

By

George Mikeal Gateau III

Thesis submitted to the Faculty of the Graduate School of the

University of Maryland, College Park, in partial fulfillment

of the requirements for the degree of

Master of Science

2011

Advisory Committee:

Assistant Professor Sarah Bergbreiter (Chair)

Assistant Professor Pamela Abshire

Associate Professor Nuno Martins

Assistant Professor Nikhil Chopra

Dedication

To my family, my grandparents, and my girlfriend

For the love and support they have given me.

Acknowledgements

I would like to thank my advisor, Professor Sarah Bergbreiter, for the amazing amount of help she has given me. She has helped me throughout my graduate career, from course work to designing the PCBs of TinyTeRP. I am very fortunate to have had her as an advisor.

I would like to thank Professor Pamela Abshire, Professor Nuno Martins, and Professor Nikhil Chopra for their expertise and guidance throughout the TinyTeRP project and serving on my examination committee.

I would like to thank the graduate students of MRL; Aaron Garrett, Ivan Penskiy, and Dana Vogtmann, for their expertise and advice during this work. I would also like to thank the undergraduates, Daniel Mirsky, Andrew Sabelhaus, and Maxwell Hill for their time and dedication to the TinyTeRP project. I would also like to thank William Pappas for advice and critiques during the creation of TinyTeRP.

Table of Contents

List of Tables

List of Figures

Chapter 1 Introduction

In the last century robots have become an integral part of life. A robot, for this research, is a device that has the ability to perform tasks repetitively. Robots can complete tasks from assembling cars to cleaning floors. These robots can be found in various sizes, ranging from several meters to millimeters in length. Small robots are capable of completing tasks that larger robots cannot, such as scurrying under doors and stealthily moving from place to place.

These small robots can be broken down into groups based on their size. This paper will focus on two sizes; centimeter robots (centi-robots) and millimeter robots (milli-robots). Centi-robots have characteristic feature sizes of centimeters and volumes of several or more centimeters. Milli-robots have characteristic feature sizes of millimeters and volumes from 1.0 cm^3 to several mm^3.

Robots can also be described as autonomous, mobile, smart, non-tethered, etc. This work will focus on centi/milli autonomous smart un-tethered mobile robots Autonomous will refer to a robot that can perform tasks without human intervention and have self contained sensing and control. Mobile robots will refer to robots that can move the entire robot from one location to another. Smart robots have the ability to sense and make decisions based on its environment. Non-tethered robots will not be linked to an external power or control unit to operate.

1.1 Applications for Small Autonomous Robots

The main reason for creating the small robot in this paper is for further research with small robots, such as fabrication, control, actuation, sensing, etc. There

can be many interesting applications for small robots excluding research. It would be most useful to use these small robots to their advantage, which is size, cost, stealth and swarm applications. These robots can reach places larger robots cannot and a larger number of smaller robots can be used in a small area. Using many small robots can increase their versatility with the use of different sensors outfitted on the robots. The different sensors on different robots could collect more data measuring different stimuli.

One application for small robots is data collection in hazardous environments. The hazardous environments could include nuclear fallout, such as the disaster of Three Mile Island and more recently the reactors leaking in Japan, to visual images inside of a locked hazardous room using a camera. This could eliminate human workers that would have to otherwise go into the hazardous area. The use of hundreds or thousands of robots could spread throughout the area and relay information back to a base station, which would be very beneficial to the workers. If the area is too large for direct communication back to the base station, then robots could hop the message back to the base station.

Spy applications are another area where size, costs, and stealth are important. A well known military spy robot classification is the Unmanned Aerial Vehicle (UAV). UAVs fly in the air and send information, such as images, back to a base station. In addition to UAVs there is Unmanned Ground Vehicles (UGV). These robots are usually hundreds of centimeters or meters in size. The military is currently testing the usefulness of a Small Unmanned Ground Vehicle (SUGV), the XM1216 [1], [2].

Another classification of military robots is called Micro Unmanned Ground Vehicles (MUGV). SUGV and MUGV could be a great addition to the military's arsenal.

1.2 Literature Review: Centi and Milli Robots

The centimeter scale will refer to robots with a volume of several or more centimeters cubed and lengths and widths of several centimeters. There have been many robots built by various designers at the centimeter scale. Each robot is often built tailored to the designer's objectives, goals, and motives for building the robot. These robots come with a variety of design choices including: locomotion methods, data processing capabilities, and sensor payloads. Depending on the intended application, these design choices will affect the final configuration of the robot.

Millimeter scale robots are robots with volume of mm^3 and feature sizes of millimeters. Some of these robots have to be tethered due to the inability to supply enough power on board to actuate the robot. Also, these robots often use actuators that require high voltages, >100 V, which introduces a challenge since most microcontrollers and lithium ion batteries supply 3.5 V.

1.2.1 Centi-robots

One example of a centi-scale robot is ALICE from EPFL, shown in Figure 1.1 [3–5]. Alice is approximately 2.0 x 2.0 x 2.0 cm (8.0 cm^3). Alice is a robot with a reconfigurable base module, watch motors with aluminum wheels for locomotion, and button cell batteries for power [4]. The designers of ALICE decided to use infrared (IR) transceivers for both obstacle detection and short range communication

[5]. IR transceivers send and sense IR light. IR transceivers are convenient because the same sensor can be used for two purposes, IR obstacle detection and IR communication. IR communication has several challenges including extremely short range, about 4 cm, and low data transfer rates [5]. A separate radio module was available for ALICE that used an 868 MHz transceiver, which could send and receive 868 MHz radio transmissions. This transceiver used more power than IR; transmit power increased from 3 mW for IR to 24 mW for the radio. The tradeoff for an increase in power consumption was a increase in communication distance. The radio module also added height to ALICE's platform, increasing the overall volume from approximately 8.0 cm^3 to 10.0 cm^3. Exact dimensions were not given but it appeared that ALICE grew larger with each additional sensor module and larger locomotion platforms. Several revisions were made to ALICE which included a rechargeable NiMH battery, various wheeled locomotion devices, and different sensor payloads [5].

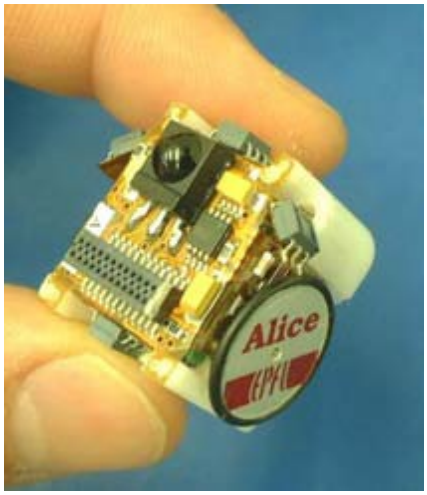

Figure 1.1: ALICE in 2002 [3]

RoACH is another example of a centi-robot designed by Dr. Fearing, shown in Figure 1.2 [6], [7]. This robot is approximately 3.0 x 3.0 x 2.0 cm (18 cm^3). RoACH's locomotion is achieved by using bio-inspired legs. One challenge for RoACH was using Shape Memory Alloy (SMA) for its actuator. SMA was chosen for its high force density and ease of assembly. However, the SMA actuators use over 0.8 W of power when actuated and have slow response times due to heating and cooling SMA. A DC-DC step-up module was used to increase the battery voltage from 3.7 V to 13.6 V needed to properly actuate the SMA. RoACH also uses IR for communication. Combined with a legged platform, the robot moved slowly, roughly 3 cm/s.

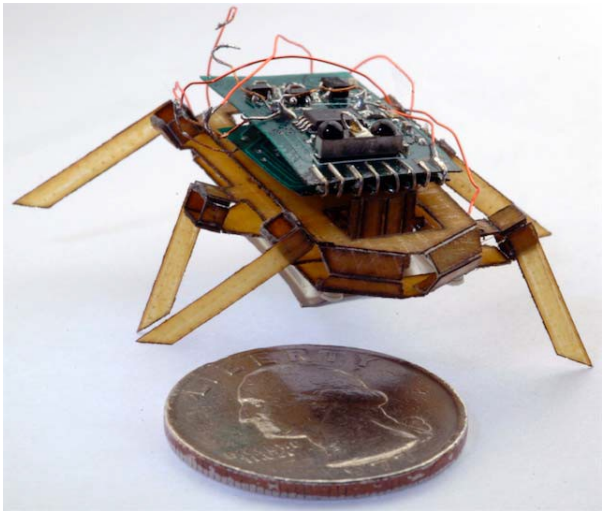

Figure 1.2: RoACH standing next to a U.S. quarter [6]

The Kilobots are relatively new robots, appearing in 2011, from Harvard, shown in Figure 1.3 [8] . This robot has a circular platform with a diameter of approximately 3.0 cm and a height of 3.5 cm (25 cm^3). A few interesting design choices made with attention to the challenges of using numerous robots. For example, an over head IR programming device can program large numbers of Kilobots at once.

Charging of the Kilobot's lithium ion polymer battery is done collectively, which decreases charging time compared to charging a large number of robot batteries independently with a single charger. Each Kilobot costs about $14.00 total, which is the least expensive robot available by $120.00 [8]. One limitation of this robot is using IR communication because IR's short communication distance. Another limitation of the Kilobot is using vibrating legs for locomotion. The vibrating leg locomotion limits the robot to extremely smooth surfaces.

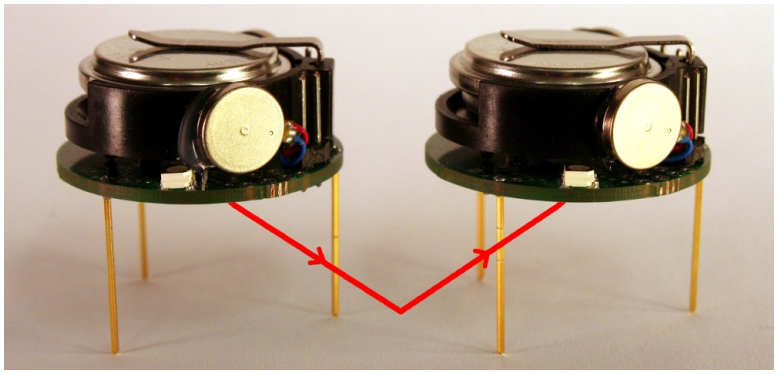

Figure 1.3: An illustration of two Kilobots communicating [8]

HAMR^3 is a third generation autonomous hexapod by Dr. Wood, shown in Figure 1.4 [9]. HAMR^3 is approximately 4.0 x 2.0 x 1.5 cm (12 cm^3). The robot can move with an average speed of 3.0 cm/s using a six leg platform with piezoelectric actuators. Piezoelectric actuators create a mechanic stress when voltage is applied, actuating the legs. This voltage is usually high and in the case of HAMR^3 a custom circuit was needed to step 3.7 V up to 200 V. This high voltage presents a challenge because most rechargeable batteries store less than 5.0 V and integrated circuits often use less than 5.0 V.

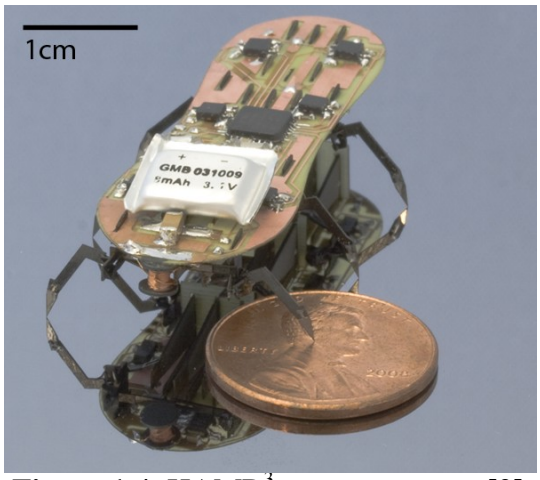

Figure 1.4: HAMR^3 next to a penny [9]

Table 1.1: Comparison of Centimeter Scale Robots ([4], [6–9])

Robot Name	Size (cm^3)	Comm. Type	Locomotion	Actuator	Speed (cm/s)
Alice	8	IR	Wheel	DC motor	?
Roach	18	IR	SMA	SMA	3
KiloBots	25	IR	Stick Slip	DC motor	1
HAMR3	12	None	Legs	Piezoelectric	3
This Work	8	RF	Wheel	DC motor	20

1.2.2 Milli-robots

A tethered walking silicon milli-robot was created by Ebefors, shown in Figure 1.5 [10–12]. This robot is approximated to be 1.0 x 0.7 x 0.5 cm (0.35 cm^3). This robot could achieve locomotion speeds of 0.6 cm/s and the ability to lift loads 30 times its own weight. The robot was created by etching "V" shaped grooves into silicon. Polyimide was then deposited into the grooves which allowed greater expansion in the wide portion of the groove than the narrow portion. The expansion was caused by joule heating which occurs when current flows through a conductive medium, in this case through doped silicon heaters. The increase in temperature

causes polyimide to expand and the expansion causes the leg to move. One challenge when using thermally actuated legs was large power consumption, this robot used 1.1 W when walking at maximum speed. To supply this large amount of power at this scale, the robot had to be tethered for powere and control using bond wires.

Figure 1.5: Walking silicon robot by Ebefors [10]

Churaman, of the University of Maryland, created the first autonomous jumping energetic porous silicon robot, shown in **Figure 1.6** [13–16]. This robot was approximately 0.7 x 0.6 x 0.7 cm (0.3 cm^3). Non-tethered jumping locomotion was demonstrated by using a phototransistor to trigger an energetic nanoporous silicon reaction and propel the robot into the air. Power for the circuit was stored in a capacitor on top and porous silicon was attached to the bottom of the robot platform. One challenge for the use of porous silicon is water absorption from humid air. Another challenge is the limited jump cycles that the robot can perform.

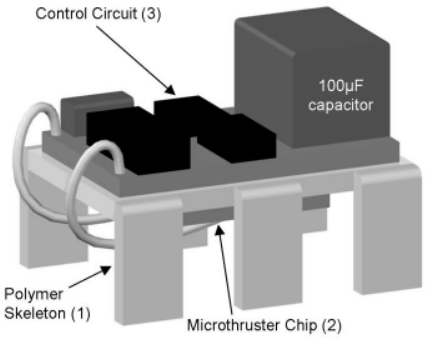

Figure 1.6: Porous Silicon Jumping Robot Courtesy of Wayne Churaman [13]

A flying robot was created by Dr. Robert Wood of Harvard, shown in Figure 1.7 [17], [18]. This robot, with wings, is approximately 3.2 x 0.5 by 0.3 cm (0.48 cm^3), classifying it as milli-bot for this paper. The robot uses a piezoelectric actuator and transmission to flap wings. The actuator and transmission are created using smart composite microstructures (SCM) [19], a process that allows scalable micro-structures to be created quickly. The robot was able to achieve flight using off board power and control. One challenge for this robot is the use of piezoelectric actuation, which needs high voltages to operate, 300 V. Another challenge is flight stability, which is currently provided using guiding rods and off board control.

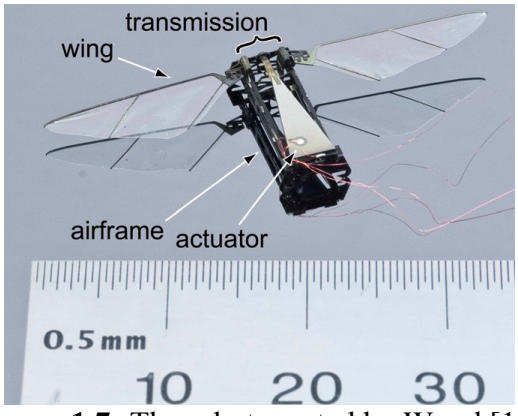

Figure 1.7: The robot created by Wood [17]

Table 1.2: Comparison of millibots

Robot	Size (cm3)	Power	Control	Locomotion	Actuator
Ebefors	0.35	tethered	tethered	legs	Thermal
Churaman	0.3	on board	on board	jumping	Energetic silicon
Wood	0.48	tethered	tethered	flying	Piezoelectric

1.2.3 Literature Review Conclusions

While not every robot was analyzed, most centimeter robots use IR communication, which has a short communication range. These centimeter robots are also generally larger than 10 cm^3 and are expensive to make, with the exception of Kilobot. Millimeter robots often use off board power and control. This limits the ability for autonomous robot control because the robot has to be attached to a stationary device.

Chapter 2 TinyTeRP

The robot introduced in this paper is called the Tiny Terrestrial Robotic Platform, or TinyTeRP for short. TinyTeRP is a step in the process of creating a milli-scale robot. This research was completed as part of Antbot at the University of Maryland, College Park; a collaborated project between multiple departments that started in the Fall of 2009. Of interest to Antbot is creating actuators and platforms for centimeter and millimeter scale robots. Work in the Antbot group includes designing time difference of arrival (TDOA) distance measuring devices [20], control algorithms [21–23], actuators [24], [25], and several other projects. To be useful to the Antbot group a few key parameters were addressed. These parameters are:

- **Size**: Hundreds of small autonomous robots will fit within 1.0 m^2.
- **Cost**: Will have an effect on the number of robots built with a reasonable amount of money.
- **Fabrication Time**: Will influence the number of robots that are able to be built in a reasonable amount of time.
- **Reconfigurability**: Will allow different sensor, actuator, and robot configurations to be studied working together in a collective group.
- **Communication**: The robots will need to communicate to other robots and computers.

2.1 Design Goals

TinyTeRP began with six goals, the first being size. TinyTeRP would also have to contain locomotion, energy, sensors, and control boards while remaining small.

TinyTeRP's target size was set at 1.0 cm^3 because it would break into milli-robot size. These included the surface it would operate on, the environment it would operate in, and the duties that TinyTeRP was to perform. It was assumed that TinyTeRP would operate on smooth surface such as tile. The tile surface in the Antbot lab rarely has obstacles more than 0.1 cm in size, excluding tables, chairs, etc.

The second goal was the final cost of the robot, including parts for locomotion would be under $50.00 which would allow 100 TinyTeRP robots to be built for $5000.00. To reduce cost, TinyTeRP will use products that are commercially available of the shelf (COTS), such as in [26]. If TinyTeRP has a length and width of 1.0 cm, then 100 robots could be released in a 1.0 m^2 area with only 1.0% being filled. For swarm behavior research having hundreds of robots would be beneficial and the cost of each robot would most likely be the limiting factor in acquiring hundreds of robots.

Using little power is the third goal of TinyTeRP. The robot should use less than 0.35 W at full power. 0.35 W of power can be provided by 3.5 V batteries with 50.0 mAh capacities discharging at 2.0 C. This means the robot should run for approximately 30 minutes, more than long enough for the Antbot group testing. The battery should be easily recharged and easily connected to TinyTeRP.

Fourth, TinyTeRP should be able to move quickly from place to place, much like a cockroach. A speed of 20.0 cm/s, ~20.0 body lengths, should be achieved. This will allow control logic to be tested in a reasonable amount of time.

The fifth goal for TinyTeRP is the ability to communicate over 30.0 cm away to another robot, static sensor, or computer. This would allow researchers to test dispersed swarm behavior and relay information to a computer for analysis.

Lastly, the robot should be reconfigurable. An outline for TinyTerp was created using the knowledge learned from previous robots. The robot was designed so that it would have five distant parts. The outline for TinyTeRP is shown in a Computer Aided Drawing (CAD) model in Figure 2.8. This CAD model shows a sensor module, base module, battery, chassis, and locomotion actuators. Different sensor and locomotion modules can be added to the TinyTeRP depending on the application of interest. This CAD model uses wheeled DC motors for locomotion and an ambiguous sensor module. The different sensor modules will contain different sensors and additional processors if necessary. The base module will provide the "brains" of robot, ie a microcontroller. Data will be transmitted between the base and sensor modules through a common interface that would allow multiple modules to be connected with a common header. This base module will contain a communication device, motor controllers, LEDs, and an interface for data transfer between modules. The chassis will hold the robot together, connecting the modules and battery to the locomotion actuators. In the case of Figure 2.8, the chassis would connect the modules and battery to electric motors.

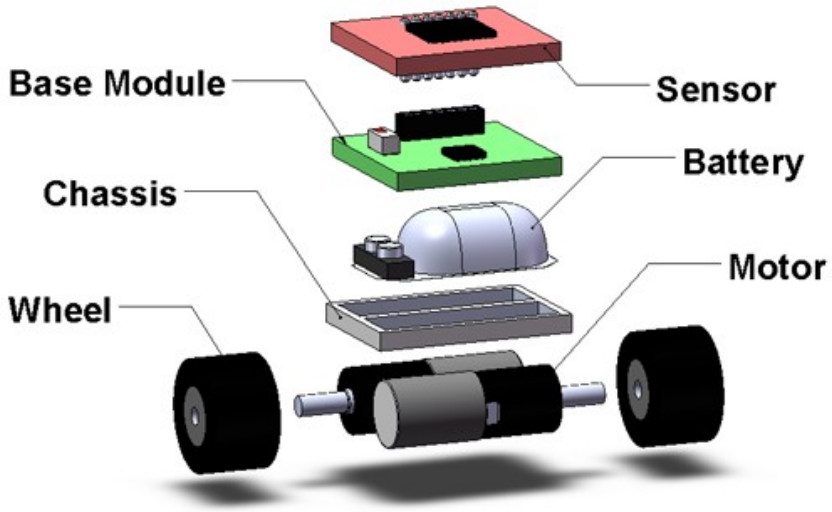

Figure 2.8: Exploded CAD view of TinyTeRP design

2.3 Battery Selection

TinyTerp will need a rechargeable small battery to power all the modules. The battery will be connected to the common header so that other modules can receive power from it. Lithium polymer batteries were chosen because these batteries can purchased as an COTS component from www.PowerStream.com. Lithium polymer batteries have a nominal voltage of 3.7 V when charged and have the ability to be recharged hundreds of times.

Unfortunately, to achieve long run times, 50 mAh batteries will be needed. Also, cheaper batteries were a priority to keep costs to a minimum. A 50 mAh rechargeable lithium polymer battery was chosen for $6.15 from www.poerstream.com. These were chosen because other websites, such as www.microflight.com, contain the same 50 mAh batteries. Table 2.3 is a comparison of a few batteries that PowerStream has available.

Table 2.3: Comparison of different lithium polymer batteries [27]

Capacity (mAh)	Length	Width (cm)	Thickness (cm)	Volume (cm3)	Cost
8	0.3	0.9	1	0.27	$ 15.00
40	0.45	1.1	2	0.99	$ 6.45
50	0.5	1.2	1.5	0.9	$ 6.15
75	0.5	1.1	2	1.1	$ 6.15

TinyTeRP needs to be rechargeable, so magnets were attached to the batteries for quick attachment. The magnets were attached by soldering the magnets to the battery leads. This is the same method used on the batteries on www.microflight.com. This allowed different batteries to be tested with TinyTeRP because changing batteries is as easy as clipping them on.

A charger from www.microflight.com was also purchased for charging the batteries. The charger can charge batteries up to 130 mAh. The charger also includes magnets so the batteries can be quickly attached. Charge times were approximately one hour.

Chapter 3 TinyTeRP's Base Module

TinyTeRP needs to be a milli autonomous smart mobile robot with the capability of making decisions. To accomplish this task, TinyTeRP will need processing, sensing, power, and locomotion. The base module will contain most of the processing and power control for the locomotion and sensing modules. This will allow for quick reconfigurability because each different locomotion and sensing module can be plugged into a common base module.

3.1 TinyTeRP Base Module Design

A few key components will be needed onboard for the base module to properly control the sensing and locomotion modules. Additionally various discrete components, such as resistors and capacitors, must all fit on a printed circuit board (PCB) with a cross sectional area of 1.0 cm^2. The components include:

- **Microcontroller:** This is an IC that contains processing capabilities along with peripheral components. Peripheral components could include operational amplifiers, analog to digital convertors, hardware multipliers, etc.
- **H-bridge:** An IC that allows a low current logic signal to control a internal circuit that will allow more current to be sourced to the locomotion module.
- **LEDs:** A programmer can use LEDs for visual feedback of the state of the base module. The LED can be switched on and off depending of sensed data, time, or state condition.

- **Header:** A way for multiple sensing or locomotion modules to be connected to one another. Also a way to program the microcontroller. The header should also include pins for serial communication between boards.
- **Radio:** The radio will allow TinyTeRP to communicate to other robots, stationary sensors, and computers wirelessly.

3.1.1 Mini-bot

Research began for the TinyTeRP base module with the creation of mini-bot [20]. This robot was approximately 6.0 x 3.5 x 5.5 cm (115.5 cm^3) and used a Texas Instrument's eZ430rf2500 (eZ430) development board. The eZ430 and locomotion module were both COTS components. A 50 mAh Full River LiPo battery was connected to a header and was used to power a eZ430 board. **Figure 3.9** is a picture of the mini-bot.

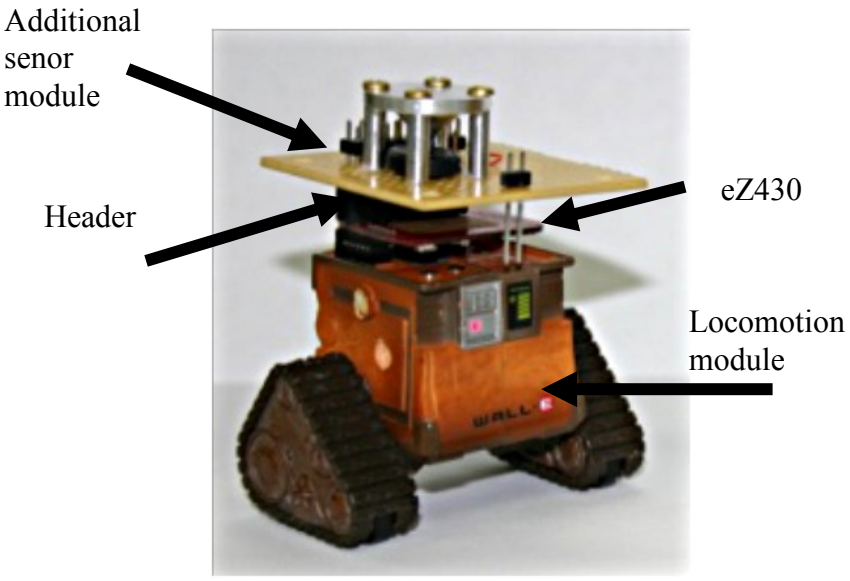

Figure 3.9: eZ430 mounted on mini-bot [20]

The base module's eZ430 target board costs $25.00 and the hardware for debugging and programming dongle costs an additional $25.00 [28], [29]. The eZ430 was chosen because it is COTS, low cost, available, well documented on the web, and shipped assembled. The eZ430 contains an MSP430F2274 microcontroller, CC2500 radio IC, LEDs, and other various discrete components necessary for the microcontroller and radio. The dimensions of the board are 2.0 x 3.0 x 0.3 cm (1.8 cm^3) and a picture of the board is shown in Figure 3.10.

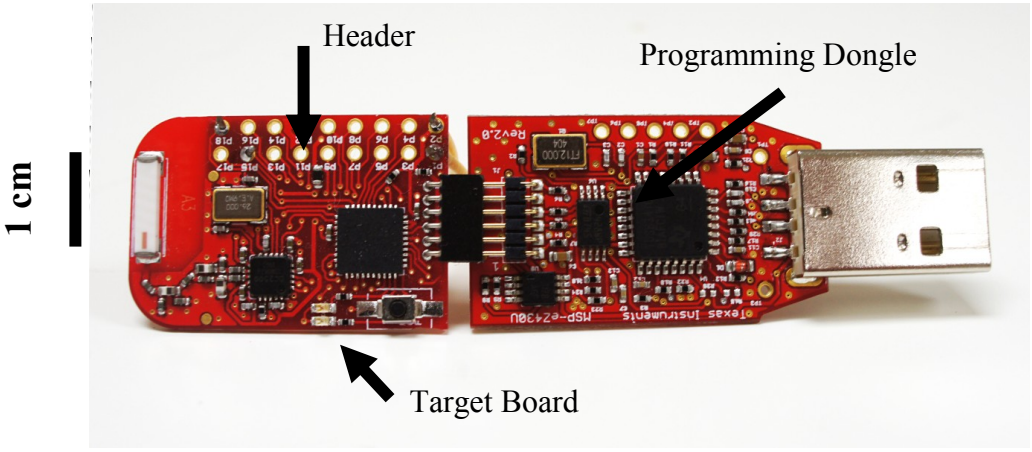

Figure 3.10: eZ430RF2500 Evaluation Kit

Limitations for the eZ430 included connecting the motors directly to the eZ430. There was a concern for circuit failure since the maximum current output of the microcontroller is only 20 mA and the motors in mini-bot used approximately 100 mA. Although, the robot was still mobile and the DC motors would run, it was decided that a better design would have an H-bridge on the base module to distribute current to the motors with control from the microcontroller.

Another limitation of the eZ430 was size. Since the eZ430 was already over the target size, it was clear that a new base module would be needed. The eZ430 was great for evaluation purposes, which is what it was designed for, but it could be made

smaller by using a four layer printed circuit board (PCB) rather than a two layer board. Components could also be placed on both sides of the board rather than one side. Extras components on the eZ430 for evaluation purposes, such as a button, 18 pin outs, and large chip antenna took up valuable space.

Serial communication ports became another limitation of the EZ430. Serial communication is a way to communicate from board to board or board to device. There are several communication techniques which include Serial Port Interface (SPI), Universal Asynchronous Receive/Transmit (UART), and Inter-Integrated Circuit (I^2C). Serial communication was supported with two sets of hardware peripherals in the MSP430F2274 microcontroller. Unfortunately the radio uses one set of these pins. This means that the radio would have to be inaccessible while another device was being communicated with causing messages to be missed. The other set of pins were routed to the 6 pin programming header and only allowed for UART communication, a serial communication method that is supported by fewer devices than I^2C and SPI.

3.1.2 PCB 1

Several revisions to the TinyTeRP base module were made. Figure 3.11 shows the progression as boards were made more efficiently. PCB 1 is the oldest board, PCB 3 is the newest, and PCB 2 is in the middle. Notice that each board becomes denser with more components being added to the boards. Also only PCB 3 has components on both sides of the board.

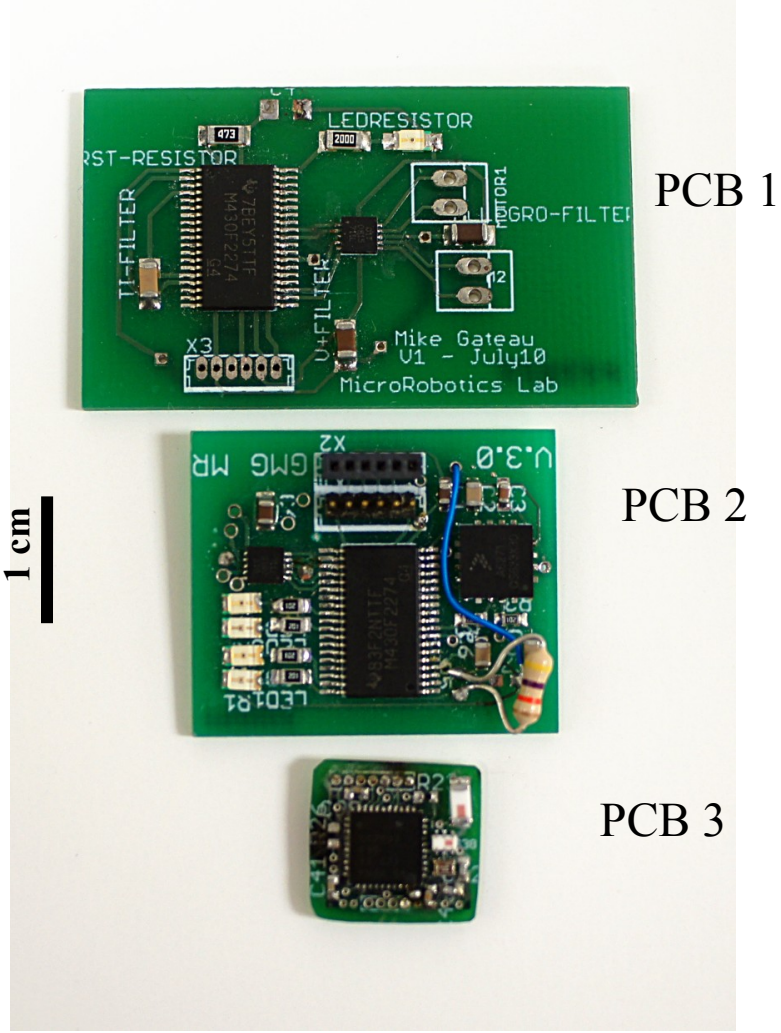

Figure 3.11: Three Revisions of Base Module (Most Recent Is Bottom Board)

The first board, PCB 1, was a two layer, one sided component board. The dimensions were 4.6 cm x 2.8 cm. This board was created to learn the ins and outs of creating a PCB. An MSP430F2274 was chosen in a plastic quad flatpack no lead package (PVQFN) because it was the same microcontroller used on the eZ430. The PVQFN package was chosen because pins were only on two sides of the package and where spaced farther apart than plastic small outline packages (PDSO). This made soldering and component placement easier.

An Allegro 3901 H-bridge was placed on the PCB 1 because it fit the requirements for the small PCB. The 3901 contained two full H-bridges and had a small form factor, 0.3 x 0.3 cm. It was also able to source 400 mA of current per H-bridge which would be enough current for 100 mA DC motors. It also operates at 3.0 V for logic inputs, and up to 5.0 V for outputs. It has a low pin count, ten pins, and pins on only two sides of the package. This allows easy soldering and placement of the H-bridge. This H-bridge was also easy to use, requiring two I/O logic pins for control [30].

Two types of headers were included on PCB 1. One header was used to connect to the motors, microcontroller, battery, and I/O devices together. This header allowed easy connection of devices by plugging into the header. The second header was a six pin header used for debugging, programming, serial communication. The pins included:

1. Receive data
2. Power
3. Microcontroller reset
4. Test
5. Ground
6. Transmit data

A LED was placed on PCB 1 mainly for debugging purposes. The LED could flash at certain frequency denoting time, progress through a program, powering up stages, etc. Various discrete components were also added such as capacitors and resistors that were needed for the msp430 and LED. Capacitors were also used for

decoupling of the msp430 from the power supply. Decoupling acts as energy sources that would filter noises and spikes in the power supply. These spikes could damage or reset the microcontroller, causes the board to fail.

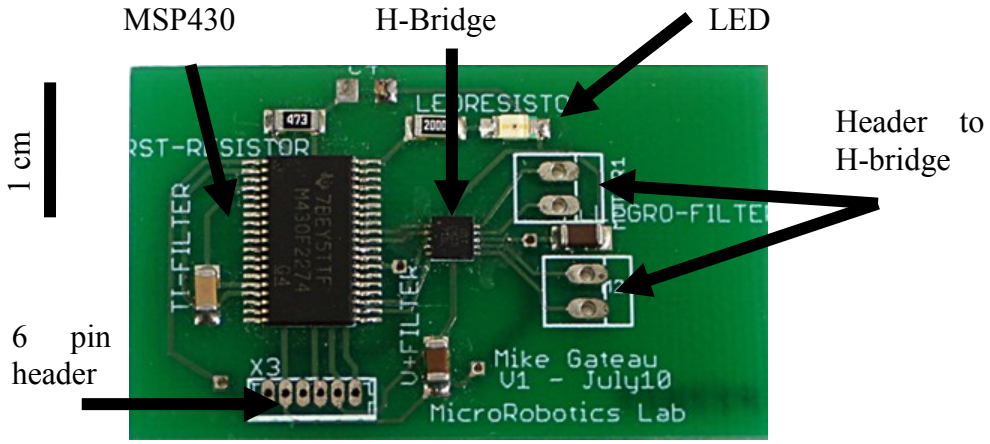

Figure 3.12: Picture labeling all the major components on PCB 1

3.1.3 PCB 2

The second board created was geared toward a smaller PCB with more functionality. The same model microcontroller and H-bridge were used again in PCB 2. In this version four LEDs were added to increase debugging capabilities. Multiple LEDs allowed for multiple visual feedback lights to be used at the same time. An analog accelerometer was also included for measuring acceleration. The accelerometer output was an analog voltage signal, so the signal was converted to digital using the analog-to-digital (ADC) inside the MSP430f2274.

The final dimensions of PCB 2 were 3.1 cm x 2.4 cm. The board and components are shown in Figure 3.13. A slight mistake was made when designing the

board that cause a pin to be connect to ground instead of power. This was fixed with a jumper wire and allowed the board to function properly.

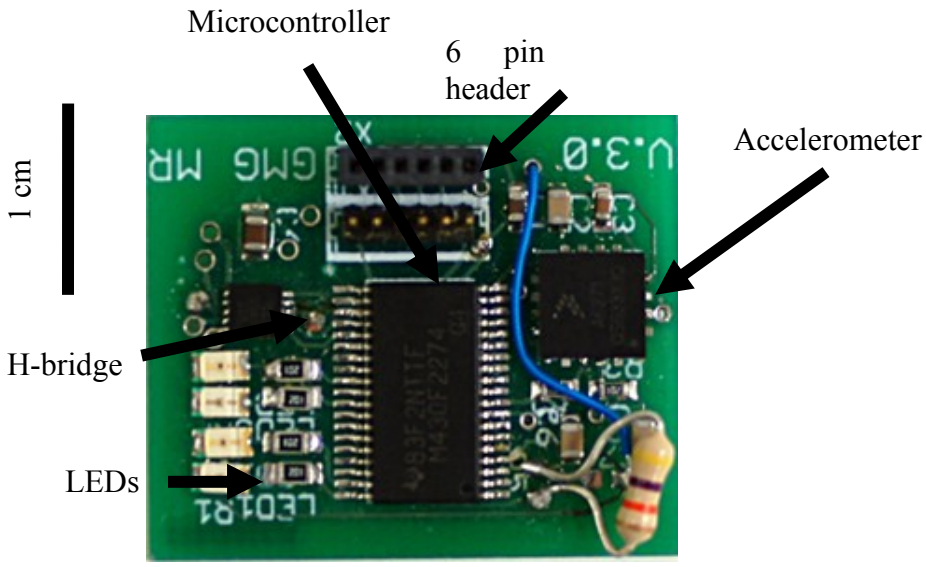

Figure 3.13: Picture of PCB 2 labeling the major components

3.1.4 PCB 3

The third and latest board, PCB 3, was entirely redesigned to be 1.0 cm^2 and have an on board radio. To further reduce size, PCB 3 was created as a 4 layer and two sided component board. Additionally a microcontroller with built-in radio, the TI CC2533 system-on-chip (SOC), was selected [31]. The decision to use the CC2533 over others was due to size, features, and availability. Other microcontrollers that included a radio were reviewed, such as the ATmega128RFA1 but were discarded due to size, cost, or availability. For example, the ATmega128RFA1's dimensions were 0.9 cm x 0.9 cm compared to the CC2533's dimensions of 0.6 x 0. 6 cm [32].

The CC2533 came in a plastic quad flatpack no lead package (PVQFN). This was chosen as it was much smaller than using other package types such as plastic small outline package (PDSO). Figure 3.14 shows the size difference between the

PDSO and PVWFN package. The PVQFN package is more difficult to solder because four sides need to be aligned increasing the chance of bridging the leads together or misalignment. Bridging of leads occurs when solder connects adjacent connections mistakenly during soldering. Misalignment occurs when the component becomes soldered to the wrong pads. Bridging and misalignment will both cause problems and the board may not work if either occurs.

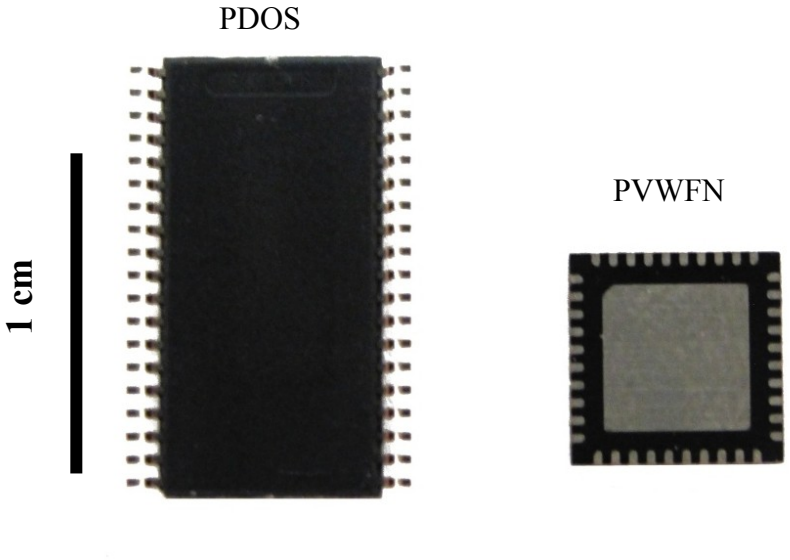

Figure 3.14: Comparison of Size Based Solely on Package Type

The CC2533 has a built-in radio and therefore requires additional components to connect the CC2533 to an antenna. These additional components were needed for all SOCs reviewed that included a radio, so the additional components were unavoidable. The additional components included a balun and crystal [33]. The use of the small chip antenna was known to decrease the efficiency of the radio and range but it was necessary to fit all the required components onto a small form factor board.

Although, packet loss (<10%) at distances greater than 20 m outdoors and several meters indoors were later demonstration on a completed TinyTeRP module.

The Allegro 3901 dual H-bridge motor controller was chosen as it was the smallest and easiest to use. The use of the Allegro 3901 allowed the microcontroller to reverse the direction the DC motor rotated. This 3901 also allowed more current to be sourced to the locomotion devices rather than the 20 mA available directly from the CC2533.

Finally, a 7 pin female header was used for serial communication between boards, as well as power and programming. The pins included power and ground from the battery, three pins for programming the CC2533, and two pins for I^2C communication. I^2C was chosen because it was available on the CC2533 and had the ability to communicate with multiple devices by using the device's I^2C address.

Basic resistors and capacitors were also included on the board that were needed for the ICs and for power decoupling. These discrete components come in standard sizes. A short comparison of sizes can be seen in Table 3.4. 0402 standard size packages were chosen because the resistors are placed with tweezers onto the base module because 0201 were determined to small for reflow soldering by hand placement.

Table 3.4: Comparison of different standard discrete component sizes

Package	Length (mm)	Width (mm)	Power Rating (W)
201	0.61	0.30	0.0500
402	1.00	0.51	0.0625
603	1.60	0.79	0.0625
805	2.00	1.30	0.1000

The final cost of the base module is $19.28. Table 3.5 breaks down the cost of the base module. The CC2533 is the most expensive component, which makes up 1/3 of the final cost. All the components, except for the PCB, are COTS and available of www.digikey.com.

Table 3.5: Cost of all components on PCB 3

Base Module Cost			
Part	**Quantity**	**Cost**	**Total**
Resistors	4	$ 0.05	$ 0.20
Capacitors	6	$ 0.05	$ 0.30
Crystal	1	$ 3.60	$ 3.60
Balun	1	$ 1.50	$ 1.50
Antenna	1	$ 1.18	$ 1.18
Headers	1	$ 3.50	$ 3.50
CC2533	1	$ 6.50	$ 6.50
Allegro 3901	1	$ 1.50	$ 1.50
PCB (large order)	1	$ 1.00	$ 1.00
Total			**$ 19.28**

3.2 PCB Fabrication

The next step in the design of the base module was to create a CAD model the base module in ProEngineer, with the all the components using the dimensions of the components. By placing and adjusting each component, it was found that the board could be made very close to 1.0 cm^2. The ProEngineer model saved time later in the board layout program because it showed whether it would be feasible to fit these components on a 1.0 cm^2 board before going onto the next step. Figure 3.15 shows

what the board would look like by recreating the components and board in ProEngineer.

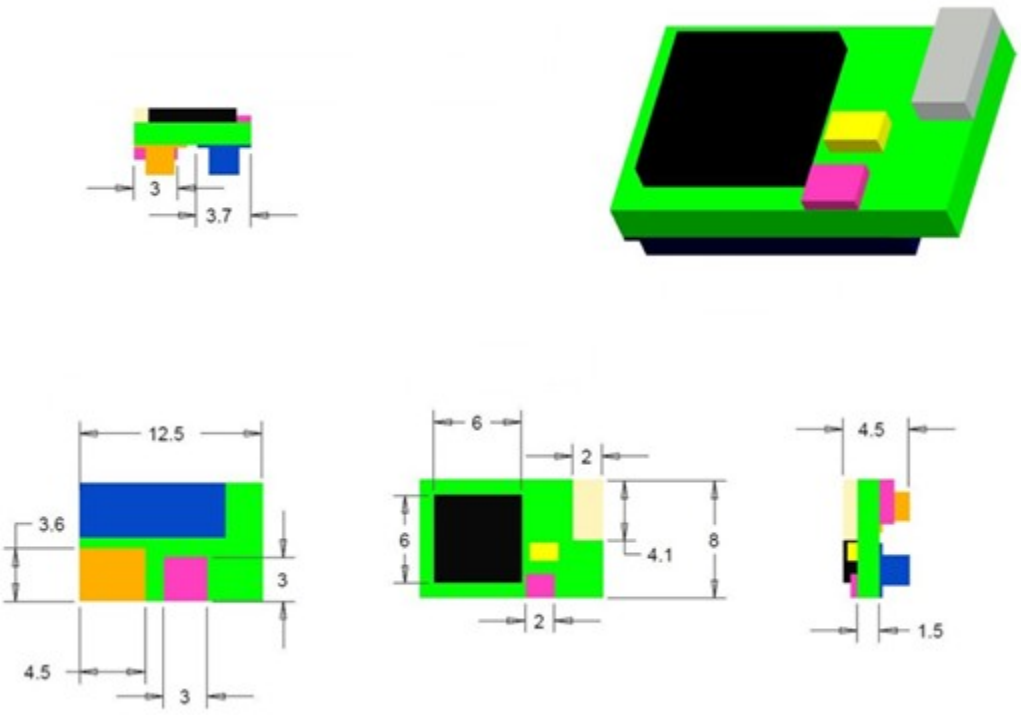

Figure 3.15: CAD drawing of base module. (Dimensions in mm)

3.2.1 PCB Creation

EAGLE was the software used to layout and route the board. Layout and routing is the process of creating the computer files needed to send to a PCB fabrication house. EAGLE is a freeware PCB designing software available for download on the web [34]. The version used was 5.11 along with the 60 day trial for creating four layer boards. Advanced Circuits, www.4pcb.com, was used as the

fabrication house for the PCB. Advanced Circuits was used because of the quick turnaround time, customer support, and inexpensive fabrication prices.

Advanced Circuits set certain limitations on the board design. These rules affected the minimum board size. For example, Advanced Circuits required 6 mil line and space along with 20 mil drill holes. The use of four layers allowed for a ground and power plane, but micro vias were not permitted [35]. These rules bumped the design from target 1.0 cm x 1.0 cm to 1.2 cm x 1.2 cm.

The board was hand routed because it was determined that auto-routing was not taking full advantage of the power and ground plane to save space. The routing by hand took much more time but was effective and was checked by the design rule checker in EAGLE so the design rules were still upheld.

Gerber files were created once the board was routed in EAGLE. The four layer cam processing tool in EAGLE produced the GERBER files that the fabrication house uses to create the PCB. The $66.00 prototype with $50.00 step and repeat was used bring the price of board fabrication to about $116.00 without shipping. There were fourteen boards in one $116.00 order, so the cost of each board was less than $10.00.

3.2.2 PCB Component Population

Populating the PCBs and other reflow soldering started with 63%Sn / 37%Pb, as seen in Figure 3.16, because it has a low melting point of ~183°C. To apply the solder paste to the PCB 3, a stencil was made from the gerber board files. The stencils were made by cutting 3M transparency film in a Versa laser cutter on low power. The steps to make the stencil are as follows:

1) Open up board in eagle.
2) Display only the layers you need (Usually tCream and bCream)
3) Use DRC to shrink Cream layers (Tools->DRC->Masks, Set Cream Max to 2-3 mil)
4) Export with CAM Processor (CAM, Device:GERBER_RS274X, Select tCream,
5) Process, Select bCream, Process)
6) Use LinkCAD to convert to DXF, follow screenshots, use Tools->Convert to outline
7) Open with DWG Editor, make sure the pads aren't filled in, scale ground pad to .5,
8) Save to DWG
9) Cut. Settings that worked: 2% Power, 12% Speed

Figure 3.16: Chipquik solder paste

After the solder paste was applied to the PCB, the components for one side were placed onto the board. The board was then placed into a toaster over and heated

to 200°C for 5 minutes. The board was then removed and allowed to cool. The board was turned over and solder paste was applied to the PCB. The components for that side were placed on and the board was once again placed in the oven and heated to 200°C for 5 minutes. The board was removed and allowed to cool.

The final board, shown in Figure 3.17, was 1.2 cm by 1.2 cm board with all components soldered on. The package was trimmed using a dremel with a cut-off wheel. The whole process took about one hour to create five boards.

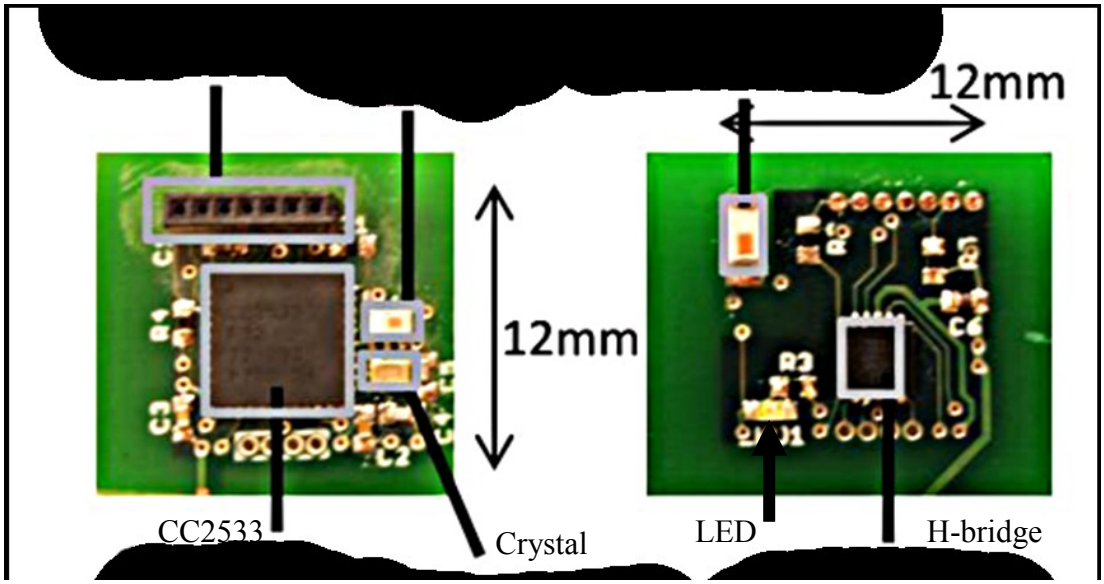

Figure 3.17: Picture labeling all the major components of PCB 3

3.3 Programming

The boards were finished by verifying every component was properly connected. The microcontroller was then programmed. The CC2533 needed a CC Debugger from TI [36] to allow the computer to flash the code onto the CC2533. The CC Debugger comes with a ten pin header that is connected to a custom connector.

This custom connector, shown in Figure 3.18, provided a place to reroute the power, ground, and debugging pins from the base module to match the CC Debugger. This connector was included in the board order to 4pcb.

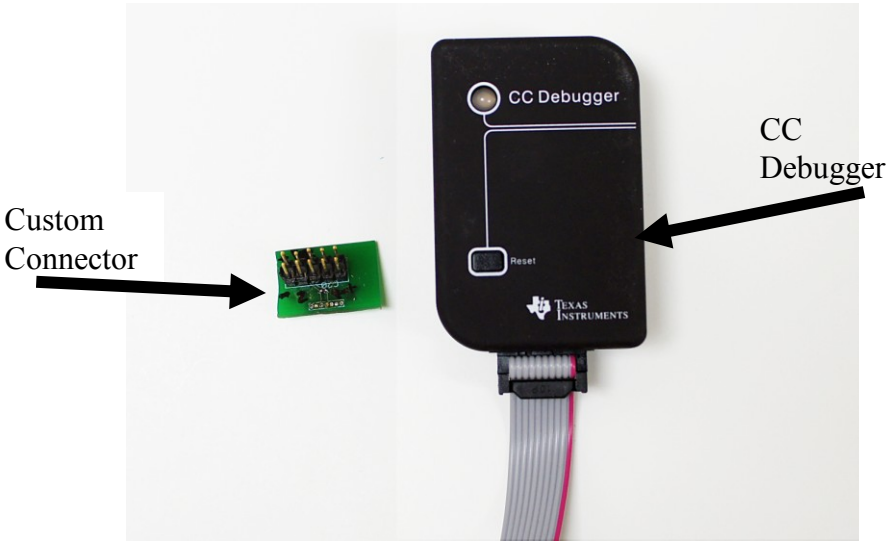

Figure 3.18: The custom connector next to the CC

The first test was a simple code that blinked the LED. Once it was determined that the CC2533 and LED were working properly, a program used the radio to send and receive a known payload. A TI sniffer [37] for the CC2533 series chips was used to determine the radio packet error rate; the sniffer is discussed further in appendix A. An arbitrary payload success rate of 90% was used to categorize working boards when placed 1.0 m away from the sniffer. It was found that most the boards, with the exception of a few, worked without any errors. The boards that did not work usually had some bridging between pads.

3.4 TinyTeRP Base Module Summary

TinyTeRP went through an iterative design process to reach the current base module, PCB 3. Learning along the iterative process, the PCB 3 uses a CC2533

system-on-chip with built in 8051 processor and 2.4 GHz 802.15.4 radio. The base module also includes an Allegro 3901 H-bridge to drive the locomotion devices, like DC motors. A header was included that allowed power to be transmitted between modules and serial communication with I^2C. The components were soldered on PCB 3 and PCB 3 had final dimensions of 1.2 cm by 1.2 cm. The on board wireless radio allowed PCB 3 to communicate to other devices and a computer with a reasonable success rate, greater than 90%.

Chapter 4 Locomotion Module

There are several ways for locomotion that could be used on TinyTeRP. The robot could use wheels to roll or legs to walk like many insects and animals. Legs can have a variety of designs, such as stick-slip [8] or whegs [38]. Whegs have the advantage over wheels for climbing over large obstacles, like legs, with speeds closer to wheeled designs.

TinyTeRP could use wings to allow the robot to fly, such as [17]. Jumping could be another method of locomotion, such as [15]. Weight is an issue with winged and jumping robots to be able to achieve lift off, but allow the robot to surmount large obstacles.

Two different approaches to locomotion, wheeled and legged, that can be used on the TinyTeRP will be discussed, shown in **Figure 4.19**. The choice for the first TinyTeRP platform uses wheels and DC motors, similar to ALICE [3–5], because of availability, large selection, and efficiency.

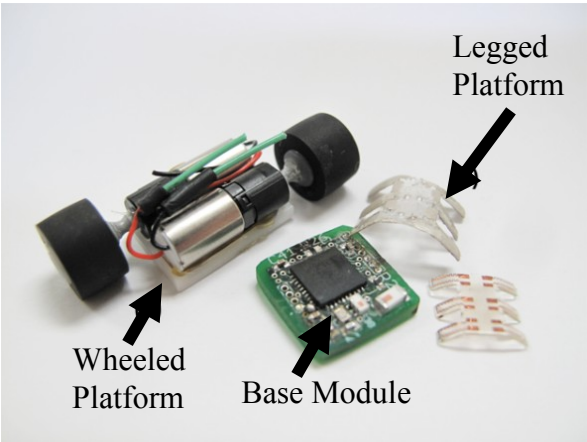

Figure 4.19: Comparison of Wheeled versus Legged Platform

4.1 Wheeled Locomotion

Wheels can surmount relatively large obstacles proportional to their radius unlike stick-slip methods that are usually limited to very smooth surfaces. DC motors and wheels are also available as COTS components, reducing price and increasing availability. Two common types of DC motors are brushed and brushless motors. Brushed motors operate with an applied voltage. Brushless motors need to be controlled using some type of feedback for proper operation. Brushed DC motors were chosen over brushless motors due to ease of use.

4.1.1 Motor Selection

There were several motors to choose from, but after sorting for redundancy, cost, and functions, three motors were chosen that were small and can run between 2.0 and 5.0 V DC. Figure 4.20 shows the three motors side by side. Motors 1 and 3 were not geared while motor 2 had a planetary gear head. Motor 2 was chosen and purchased so that no gear assembly was required. A disassembled geared motor, Motor 2, is shown in Figure 4.21. All three can be purchased from www.solarbotics.com or www.gizmozone.com.

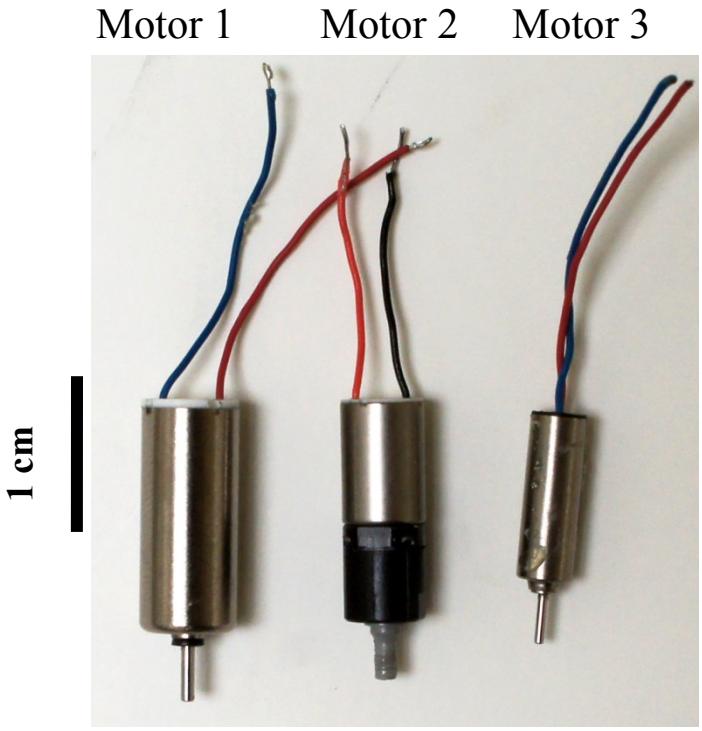

Figure 4.20: Comparison of three DC motors for TinyTeRP

Figure 4.21: Planetary Geared Pager Motor Disassembled

Motor 2 ($15.00) was more expensive than both the non geared motors (<$5.00) but provided more torque. Despite the cost, the geared motor was chosen as it made assembly of the robot easier and allowed the wheels to be directly attached. The prices and sizes of the three motors can be seen in Table 4.6. Motor 1 and 3 were tested because they were inexpensive, but it was determined that motors 1 and 3 would need gearing to be properly controlled because without gearing the motors did

not provide enough torque to start the robot from a standstill. Adding gears for motors 1 and 3 was avoided at this time due added complexity and cost.

Table 4.6: Comparison of 3 DC Motors [39], [40]

Motor	Geared	Size (mm)	No Load Speed (rpm)	Torque (N-m)	Cost
1	no	7x16	18000	1.50E-04	$ 3.95
2	25:1	6x16	1000	1.50E-03	$ 15.00
3	no	4x12	20000	9.80E-05	$ 4.40

4.1.2 Wheels

The smallest off-the-shelf wheels were from Solarbotics. Even though they seem small they are relatively large, 9mm in diameter and 4mm in width. Figure 4.22 shows the wheel that was used on TinyTeRP. Glue was used to attach the wheels to the motors.

If the motors were able to reach their maximum unloaded speed of 1000 rpm, then the robot could travel up to 52.0 cm/s. Even with some loss, friction, and other effects that would not allow 1000 rpm, TinyTeRP was still able to reach speeds of 20.0 cm/s.

Figure 4.22: Wheel Chosen for TinyTeRP Wheeled Platform

4.1.3 Chassis

A chassis was created to connect the DC motors to the base module and battery. The dimensions of the chassis were large enough for motor 2 to sit partially into the chassis. This allowed two motors to be easily connected parallel to one another. Figure 4.23 is a CAD drawing of the chassis used for TinyTerp.

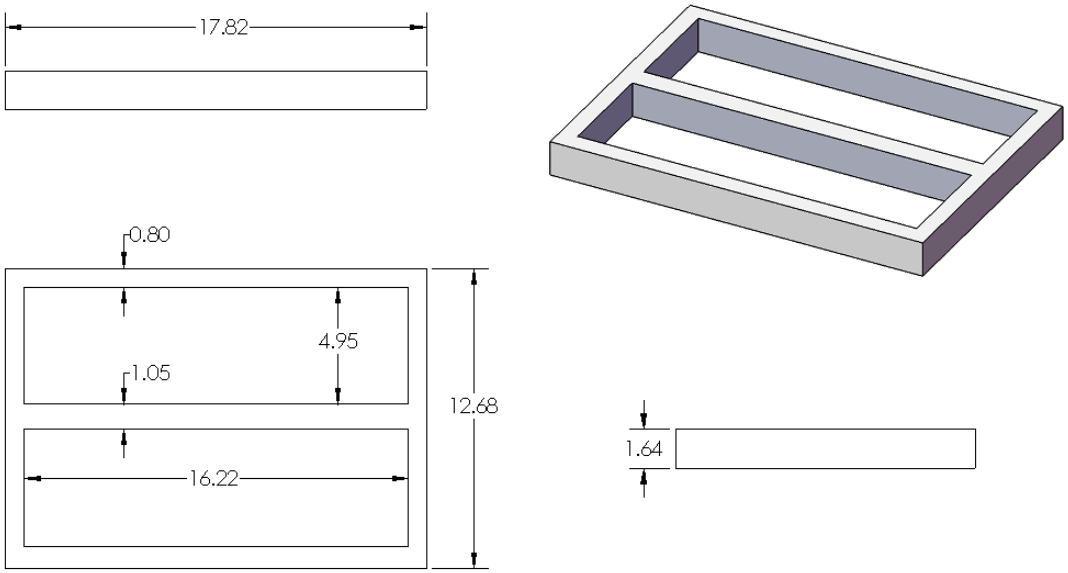

Figure 4.23: CAD drawing of the chassis (Dimensions in mm)

The CAD drawing was saved as a .DWG file to be used in a laser cutter. The material chosen for the chassis was 1.6 mm delrin, a low cost material available at www.McMaster.com. This material was known to cut well in the lab Versa laser cutter. Figure 4.24 is the chassis after being cut from the delrin. The chassis was then attached to the motors using glue. A piece of double sided tape was used to attach the battery, so that the battery could be removed easily.

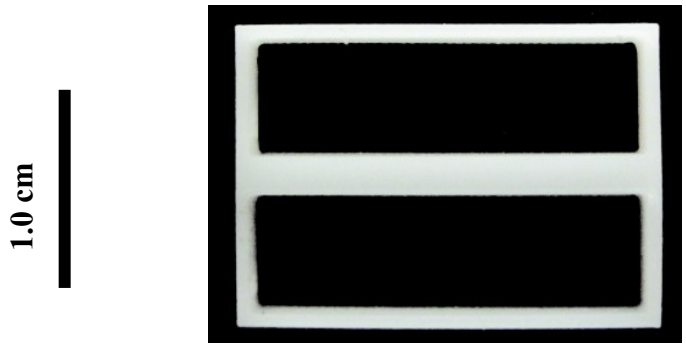

Figure 4.24: The final chassis after being cut from the white delrin in the laser cutter

4.1.4 Future Wheeled Locomotion Module

Smaller components were found through further investigation. Smaller DC motors, gears, and wheels have been found that are more inexpensive than previously thought. A new brushed DC motor wheeled locomotion module is being created that will use a smaller non geared DC motor rather than the geared motor seen previously. The new motor is 0.4 x 0.8 mm and costs $2.50. This new motor can provide 5.9e-5 N-m of torque.

Gears are needed for this new module because the motor produces low torque. Worm gears combined with spur gears were chosen for the new locomotion module because this can provide gear reduction in a small form factor. Figure 4.25 shows the worm gear and the spur gear that will be used. The spur gear cost $2.10 and the worm gear cost $2.60. This made the total cost of the new gearing and motor $7.20. This will reduce the cost of the locomotion module by $15.60 by replacing the expensive planetary geared motors.

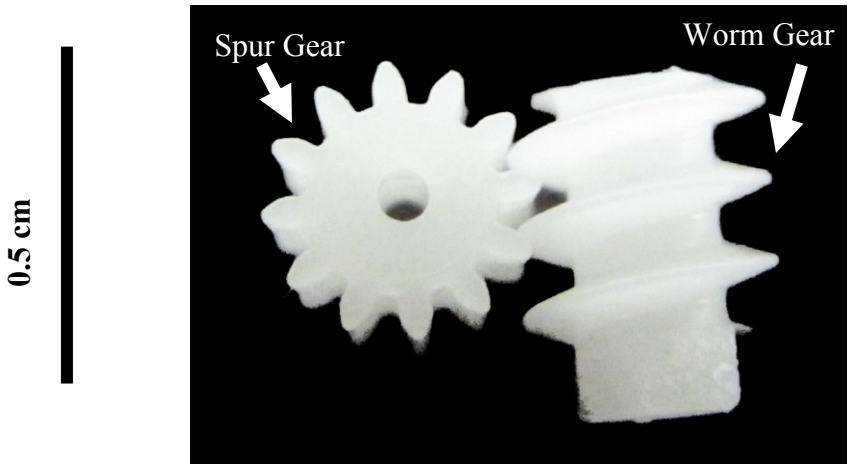

Figure 4.25: Worm Gear and Spur Gear Chosen for Newest Wheeled Platform

One of the biggest improvements will be the use of a new wheel. This new wheel is actually a o-ring made by Precision Associates, Inc. This new o-ring is 0.5 x 0.2 cm making the o-rings 0.4 cm smaller in diamter and 0.3 cm smaller in width than the old wheels. This will help to decrease the volume of the robot be removing the larger bulky wheels. Figure 4.26 shows the old wheel next to the new o-ring wheel beside .

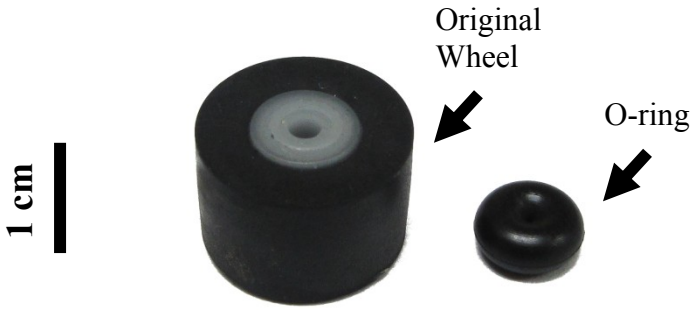

Figure 4.26: Solarbotics wheel versus o-ring

The use of gears, new motors, and wheels requires a new chassis. Unfortunately, this chassis needs to be custom made and assembled. To keep the chassis as thin and small as possible, 0.8 mm delrin from McMaster was bought. The

Versa laser cutter cut the chassis from the 0.8 mm delrin. A 0.8 mm metal rod was used as the axel for the spur gears and wheels. A CAD model of the final platform is shown in Figure 4.27.

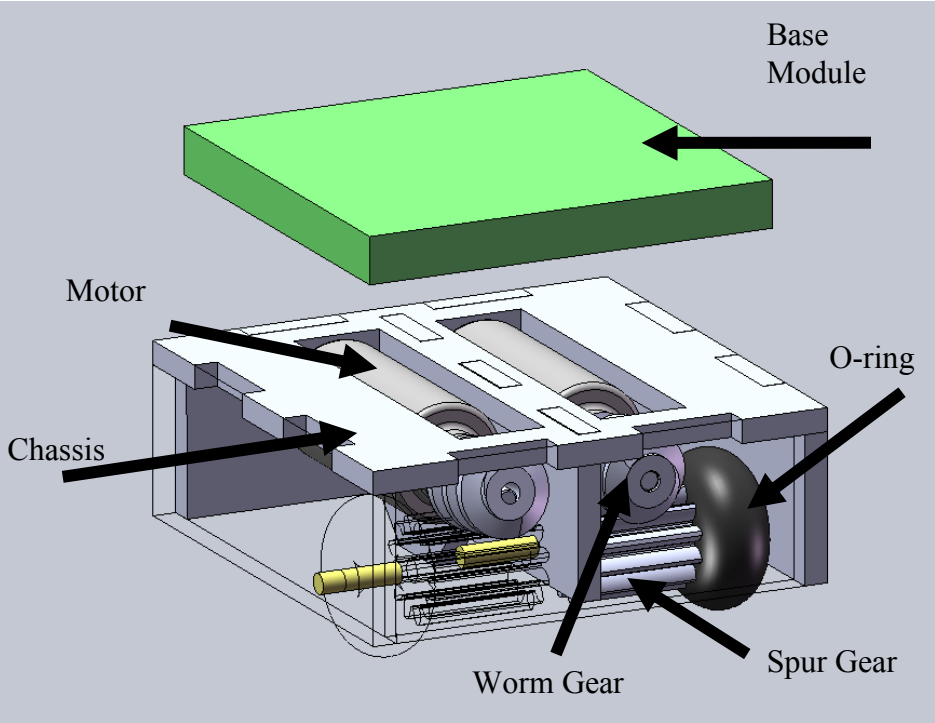

Figure 4.27: CAD of Newest Wheeled Platform created by Mr. Maxwell

This platform is amazingly 3.6 cm^3 smaller than previous chasis. The chassis also is $15.60 cheaper. The disadvatange to this design is the complexity it adds to creating the locomotion module. A thorough assembly procedure will need to be made so that each module will be made the same and to ease assembly.

4.2 Legged Platform

While the wheeled platform worked, there is interest in creating robots that are bio-inspired because it builds upon thousands of years of natural engineering and/or the ability to disguise a robot as a living biological creature. Wheels for

locomotion are not found in nature, but winged and legged creatures are very common. For TinyTeRP, having a legged locomotion platform would provide an additional module to study. Adding various locomotion methods to TinyTerp will allow researchers to experiment with different control methods because different locomotion methods interact with the environment, the robot, and control algorithms differently.

Different actuators could provide the force to drive a legged module. Electrostatic actuactors, dielectric elastomer actuactors (DEAs), piezoelectric actuactors, DC motors, shape memory alloy, and thermal actuactors are a few of technologies that could be used for a legged module.

Thermal actuators were chosen because thermal actuators can create large forces with joule heating, as seen with Ebefor's robot [10]. Another attractive quality of thermally actuated legs is the potential for low voltage actuation, as low as 3.5 V, which is already available on TinyTeRP. This is a benefit over some other actuator types that use much higher voltages, such as [9], [18], [24], [41], although electrostatic actuators are much more efficient because less power is lost through dissipated heat.

Another disadvantage of thermally actuated legs is high electrical currents and high powers used. In Ebefor's robots, 1.0 W of power was used at times [10]. Using heat for actuation has negative consequences such as slow actuation cycle speed, large current consumptions, and effects of high temperatures on the robot.

The legged research should create a millimeter scale legged platform for TinyTeRP that avoids using the clean room. The clean room adds costs, hazards,

time, and accessibility problems to the legged platform. Avoiding the clean room will help the legged platform be available to more researches and increase its ability to be studied.

4.2.1 Previous Work in Thermally Actuated Legs

Ms. Rajkowski created a polymer leg platform that used copper electrical heating elements to actuate the legs [42], [43]. The process, Rapid Microrobot Prototyping (RaMP), was proven to be cheap, fast, and precise enough for millimeter robots. Figure 4.28 shows a hexapod created using the RaMP process. Actuation was achieved by using two different materials with different coefficients of thermal expansion (CTE). This CTE mismatch causes, with an increase in temperature, one material to expand more than the other. The material with low CTE was copper and the material with high CTE was LocTite 3525.

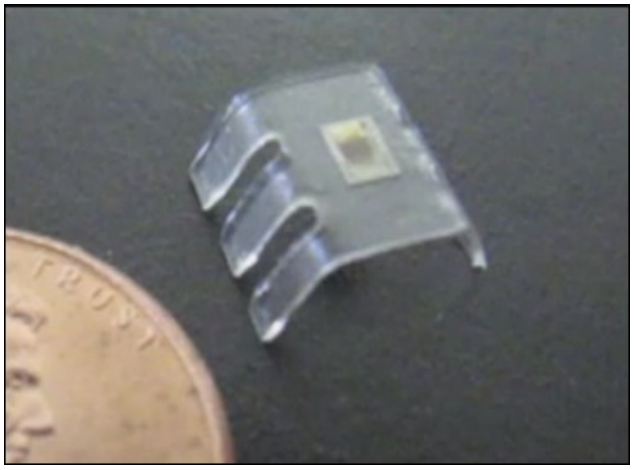

Figure 4.28: Hexapod created using the RaMP process
Courtesy of Ms. Rajkowski [44]

A Loctite hexapod was created by ultraviolet (UV) curing using a UV lamp and a mask. The mask defines which parts of the LocTite were exposed to the UV light, thus defining what part of the LocTite cured. A copper trace was then deposited by evaporating copper onto the LocTite hexapod body. Evaporation provided a very uniform thickness and width which is important to control resistance. The resistance of the copper trace was important because it is inversely proportional to the power that the heater would dissipate. The copper was the chemically etched to create heating elements. Current could then be passed through the copper trace and the leg would actuate, bending in the direction of the copper. Figure 4.29 shows the final result after the copper has been evaporated and etched. Figure 4.30 shows a hexapod with discrete components soldered on.

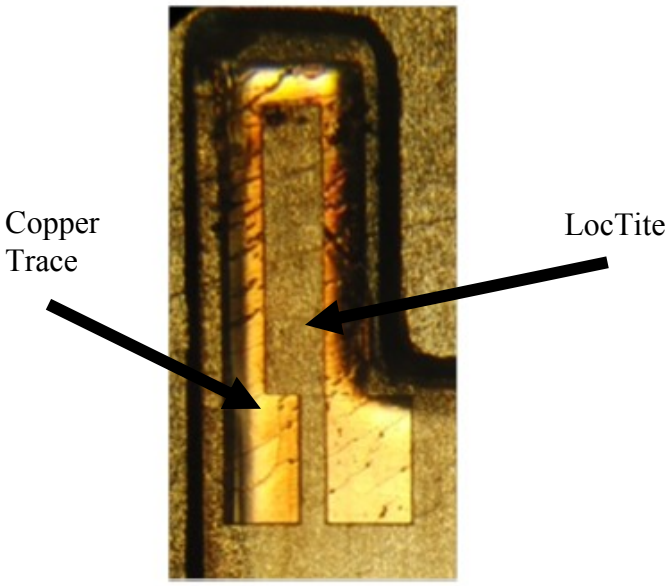

Figure 4.29: Etched Cu on Hexapod Courtesy of Ms. Rajkokswi [44]

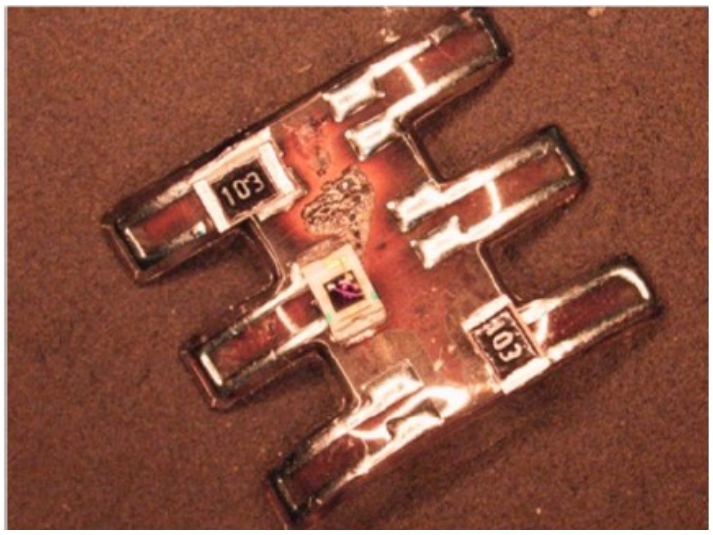

Figure 4.30: Final hexapod with components courtesy of Mr. Churaman

The RaMP process proved to be a very easy way to create a milli-robot polymer legged platform. Unfortunately RaMP still had a few challenges that restrained its use for TinyTeRP. One challenge was that the copper traces tended to crack and components were rather hard to solder on. The RaMP process also does not avoid the clean room, which some researchers may not have access to.

4.3 Thermally Actuated Legs

This research will use a similar process to RaMP but tries to completely remove the clean room. Instead of evaporating copper onto the polymer body, a thin layer of liquid conductive silver polymer adhesive is stenciled onto the polymer. This decreases fabrication time, complexity, and cost of each platform. The platform should able to be classified as a milli-robot platform, with dimensions of 1.0 x 1.0 x 1.0 cm or smaller. Displacements of 0.02 cm should also be achieved. This will allow for the actuated step sizes to be seen visually under a low power microscope.

4.3.1 Design

The leg design examined for use in the polymer locomotion platform is shown in Figure 4.31. The two layer leg uses a high CTE material as the base layer for the thermal leg. A low CTE material will be patterned on the base layer to act as a heating element.

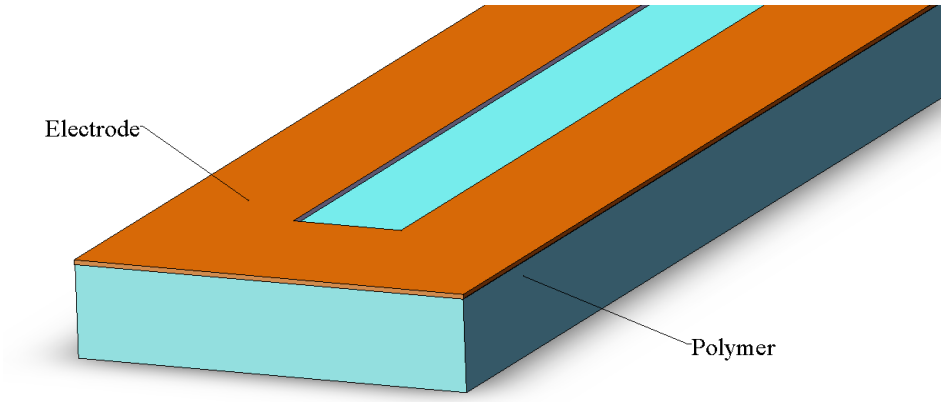

Figure 4.31: CAD Bilayer Leg Consisting of Silver Composite and Polymer

4.3.3 Material Selection

A fabrication challenge for low voltage thermal bimorph actuators is finding an electrode material that is conductive and able to be patterned. Additionally, the electrode should be able to be deposited and patterned without the use of clean room. A solution to this problem is to use a liquid conductive composite material. The composite material will have some conductive particles mixed within it.

This research used Conductive Silver 187, from www.TedPella.com, which is a liquid silver composite acrylic [45]. Sylgard 184 was used for the high CTE base

layer [46]. This polymer was used because it was readily available, easy to work with and had a high CTE. The Sylgard 184 cures in less than 1 hour on a 50.0°C hot plate. Sylgard 184 also has a viscosity low enough to create thin layers without much effort.

4.3.4 Fabrication

Fabrication of the actuators started by mixing Sylgard 184 with a 1:10 ratio as defined in the data sheet. A mold was created by placing a piece of transparency on a flat surface. Four spacers were then placed onto the transparency; the spacers will define the thickness of the actuator. The Sylgard was then poured onto the transparency, in between the spacers. A final piece of transparency was placed on top of the spacers. A flat rigid weight was placed on top of the transparency to squeeze the Sylgard to the desired thickness. The mold was then placed on a hot plate at 50 C and allowed to cure.

After the mold cured, the top transparency was removed along with the four spacers. The Sylgard and bottom transparency was then laser cut in a Versa laser to the desired shaped. The bottom transparency was then removed to leave a laser cut polymer base. A piece of Mylar was laser cut to act as a stencil for the silver composite acrylic. The silver will be brushed on the leg so the stencil would mask the area where no silver was desired. The silver composite acrylic is then allowed to cure. **Figure 4.32** shows a completed actuator.

4.3.3 Results

200 micron thick glass slides were used as spacers causing the leg to be 200 microns thick. A 12.5 micron mylar was used as the stencil creating a conductive

trace. The process took about one hour to produce an actuator, however most of the time was for the curing of the polymer. **Figure 4.32** shows the fabricated leg.

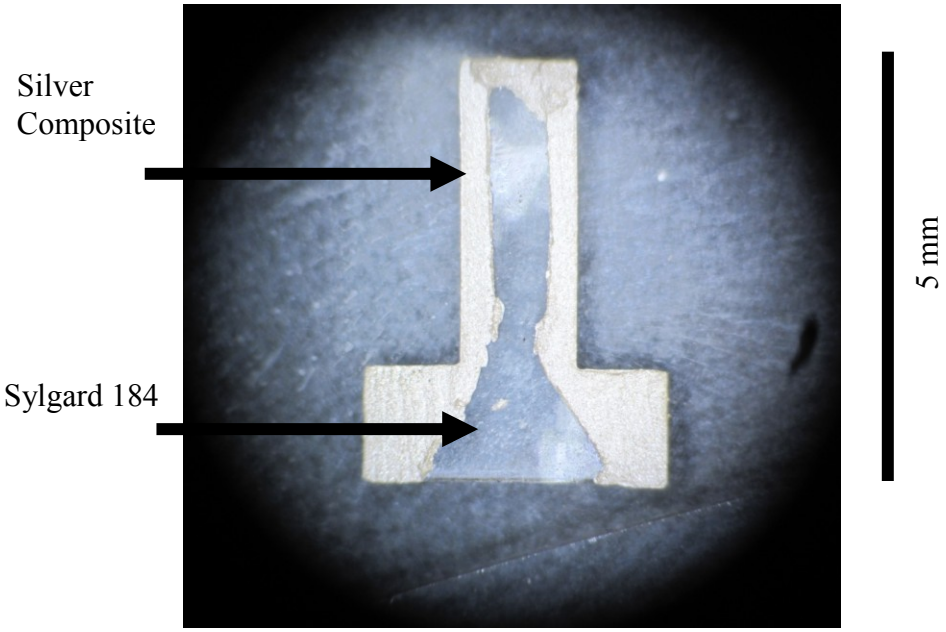

Figure 4.32: Bilayer leg after silver composite deposition

After the actuator was fabricated, current was passed through the leg. Figure 4.33 shows the leg being actuated. The left side is fully actuated by heating the electrode and the right is at room temperature. About 350 microns of displacement can be seen in the picture with 0.3 A and 1.2 V being passed through probes into the silver composite layer.

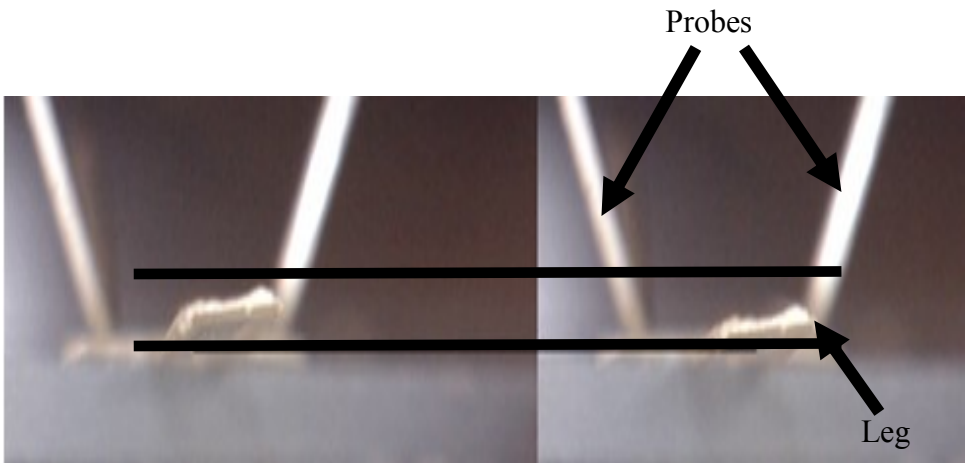

Figure 4.33: Bilayer leg being actuated

A full hexapod was not yet created due to several challenges encountered while trying to make the thermally actuated leg. One challenge was keeping the heating electrode from cracking, which created discontinuity in the electrode. Cracking was most likely due to handling and actuation. Cracking of the silver electrode occurred at times when the leg was removed from the transparency because the silver acrylic would attach to the transparency. Cracking occurred during actuation by possibly, exceeding the maximum stress and strain of the silver acrylic through actuation. The exact maximum strain of this material is not known but the strain could be reduced by a different design.

4.3.4 Future Work

A better design might be a three layer leg that has an additional middle rigid layer, as seen in Figure 4.34. This rigid layer would be thin with a low CTE. There would be a polymer base under the middle layer and the silver composite as the top layer and would heat all the layers. The CTE mismatch between the rigid layer and

polymer would cause bending towards the rigid layer. The benefit of this would be a reduction in stress in the silver composite and ease of fabrication.

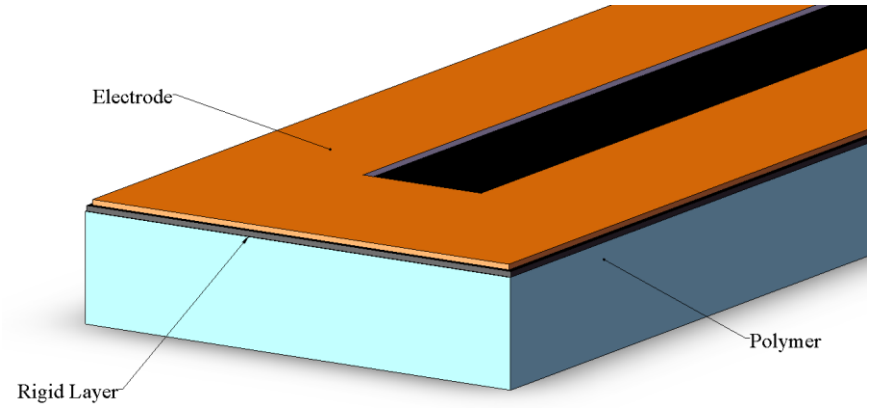

Figure 4.34: CAD Trilayer leg consisting of silver composite, thin film, and polymer

Another challenge was adhesion between the silver acrylic and the Sylgard. The Sylgard does not adhere to mylar or the transparency very well. This makes finding a COTS thin rigid layer more difficult because the Sylgad needs to adhere to the rigid layer to bend the leg. A different material, such as a urethane rubber pmc-724 [cite], might be a solution to this problem. This urethane rubber seems to adhere to material better than the Sylgard. The urethane has similar mechanical properties and preparation to Sylgard though. Both are soft, shore hardness A of ~20-40, and require two part mixing.

Chapter 5 Sensors

As stated earlier, TinyTeRP must be smart and have the ability to make decisions based on sensed stimuli from the environment. Different sensors may be needed depending on the application that TinyTeRP is being used for. For example, distance measurements will use different sensors than temperature measurements. Different sensors and applications will also require different processing resources.

Given the simple computational resources available on the base module, sensor modules with additional processing capability will be beneficial. Also, some sensors can provide some preprocessed data, such as on the IMU-6000 from invensense. The benefit of such sensors is computation time and complexity can be left to the sensor or sensor module rather than using the main microcontroller's resources.

Sensors that were considered for TinyTeRP were; infrared (IR), received signal strength indication (RSSI), time difference of arrival (TDOA), inertial measurement unit, global positioning system (GPS), touch, and optical mouse. Most of these sensors were considered because they could be used for some method of navigation control. Out of these, RSSI was the only one that could be tested on TinyTeRP due to time constraints. A mouse sensor was tested separate from the robot and an inertial sensor was created but due to time constraints was not able to be tested.

5.1 RSSI

The CC2253's received signal strength indicator (RSSI) quantifies the received power of wireless packets sent using the IEEE 802.15.4 protocol. In the ideal (free space) case, this value varies inversely with the square of distance, and consequently has been suggested as a means to estimate distances between nodes in mobile sensor networks [20], [47]. The most significant advantage of using RSSI for distance sensing is that it is already built in most radios and therefore requires no additional sensing hardware. However, recent work has showed that inherent inaccuracies of using RSSI in practical environments makes it almost useless for distance sensing without significant pre-processing or computational resources [47] In addition, since RSSI will be a function of board and antenna design, such results do not necessarily generalize across platforms.

Given the size constraints of TinyTeRP, RSSI's advantages outweigh its potential problems. In addition, most previous research focused on the use of RSSI over long distances (10s to 100s of meters) and TinyTeRP will generally be constrained to environments only meters across. Some recent work has shown better results for RSSI distance measurements over shorter distances [48]. For these reasons, RSSI was investigated to determine its performance over shorter distances. For the algorithms suggested later in Chapter 6, only an approximation of a linear relationship between RSSI and distance over 10s of centimeters is required.

5.1.1 Experimental Set-up

Two TinyTeRPs and a modified serial packet sniffer were used to determine the relationship between RSSI and distance. One of the two platforms (the sender, "TX") was programmed to transmit simple packets to the other robot (the receiver, "RX") placed a distance D away with a given orientation of the receiver relative to the transmitter. An illustration of the test set-up can be seen in Figure 5.35.

Since the software interface defined by Texas Instruments' libraries for the CC2533 provided the transmission's RSSI value as part of the receipt of a packet, the receiver repackaged that value into another transmission sent to the packet sniffer. The packet sniffer is a device that allows a computer to communicate to the TinyTeRP. Each of these two routes of communication, illustrated in Figure 5.35 operated on different channels to avoid interference.

Packets were captured from the sniffer using a serial interface on a PC while the sender TinyTeRP was incrementally moved away from the receiver. Intervals of 5 cm were used up to a distance of 20 cm, and then data were taken at intervals of 10 cm up to maximum distance of 80 cm. The PC recorded 100 data points at each distance.

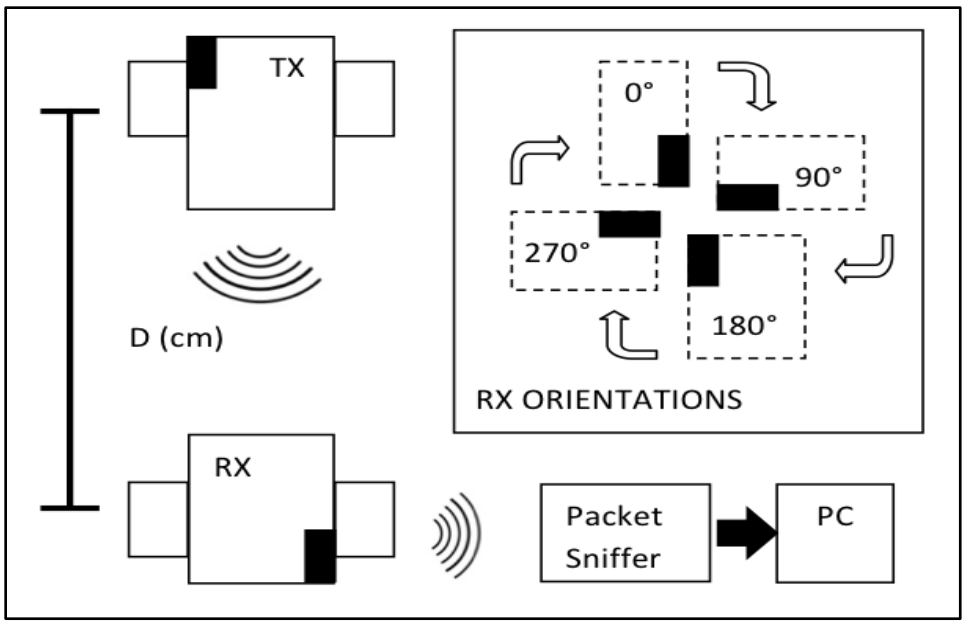

Figure 5.35: RSSI Test Setup. The orientations tested are in the upper right hand corner

5.1.2 Testing

Controlled experiments were performed to measure the dependence of RSSI versus distance with variable orientation, transmit power, channel frequency, and time.

The first test measured the RSSI value at a distance of 20cm over a long period of time (Figure 5.36). The test setup was allowed to record data until the sender TinyTeRPs' batteries were discharged. The battery power source dropped below the minimum required for the CC2533 approximately 50 minutes after the test began.

Figure 5.36 shows a very constant value throughout the test. It is important to note that the CC2533 chip minimizes the effect of a variable battery voltage on radio transmissions, which can be seen here in the constant RSSI at the end of battery life.

Slight variation only occurs in the last few transmissions, and the RSSI changes only by one unit in these cases. Consequently, it was determined that there is effectively no time-dependent noise in the signal.

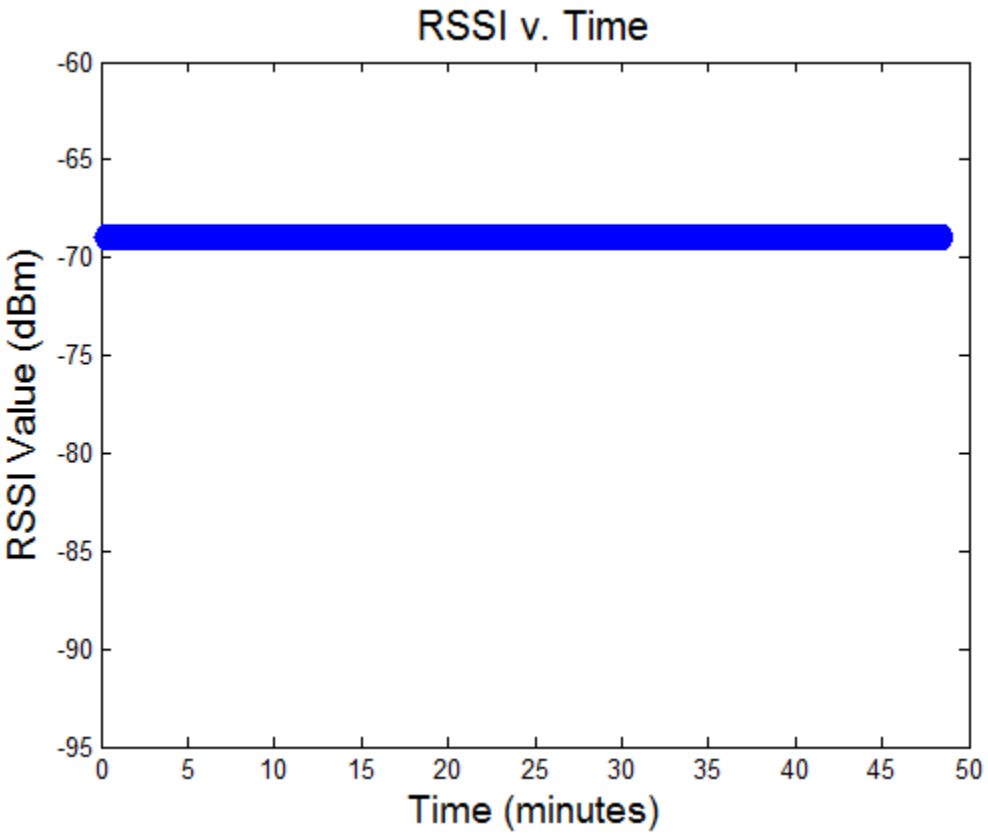

Figure 5.36: 50 minute test of RSSI at a fixed distance of 20 cm.

Next, iterative testing was performed by varying the distance between the sender TinyTeRP and its paired receiver, as discussed above. The test was repeated for three different channel frequencies with the results shown in Figure 5.37. Even though 14 different channel frequencies are allowed by the CC2533, only 5 channels resulted in successful packet transmission during pre-testing. The 2425 MHz frequency was the default setting in the libraries provided by Texas Instruments, and the remaining two frequencies were chosen to sample higher and lower bands

surrounding this default frequency. Due to the nature of the TinyTeRP's environment, ambient RF noise was expected in the 2.4 GHz range, and thus altering the transmission sub-channel could significantly affect the precision of RSSI values. In addition, the wavelength of a 2.4GHz radio transmission is approximately 12.5cm – on the same order of magnitude as the distances tested.

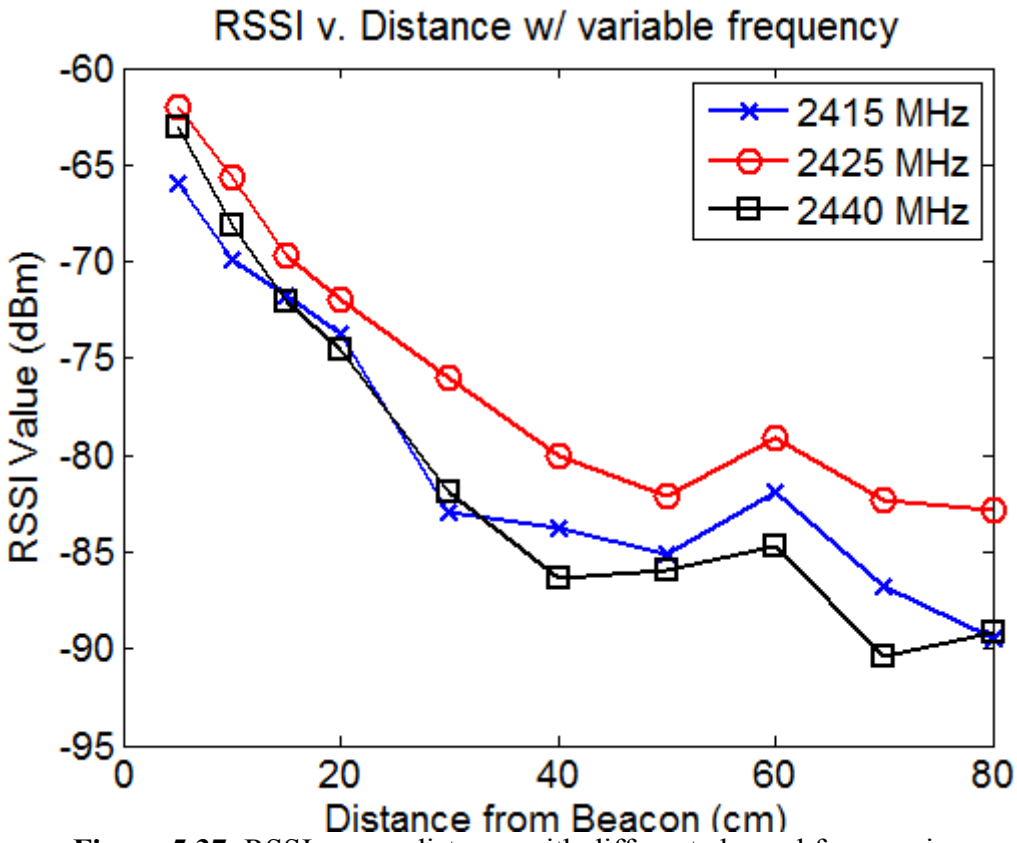

Figure 5.37: RSSI versus distance with different channel frequencies

Figure 5.37 shows a monotonically decreasing RSSI value versus distance in each of three chosen bands up to distances of 50 cm. The variability between bands is small within the first 20 cm and grows to approximately 5 dBm at greater distances. Notice that no error bars are present in these data, since the standard deviations of each set of 100 RSSI values were so small that they could not be displayed properly.

The transmission output power was also varied on the transmitting TinyTeRP and the resulting changes in RSSI were recorded. In this case, the channel was held constant at 2425 MHz and the robots' antennas were oriented along a straight line. Figure 5.38 contains data for each of three discrete transmit power levels. These transmit powers were the only available options provided for the CC2533.

It was expected that lower transmit powers would shift the curve down, but the large inconsistencies around 50 cm were not anticipated. One possibility is that some artifact of the testing setup, such as signal reflection off surrounding surfaces in the lab environment, could have contributed to the low points seen in Figure 5.38 at 50 cm when transmitting at both 0 dBm and -3 dBm. In any case, the default setting of 4 dBm resulted in consistent and usable data for the entire desired range of distances, so it was selected as the gain for future uses of the TinyTeRP.

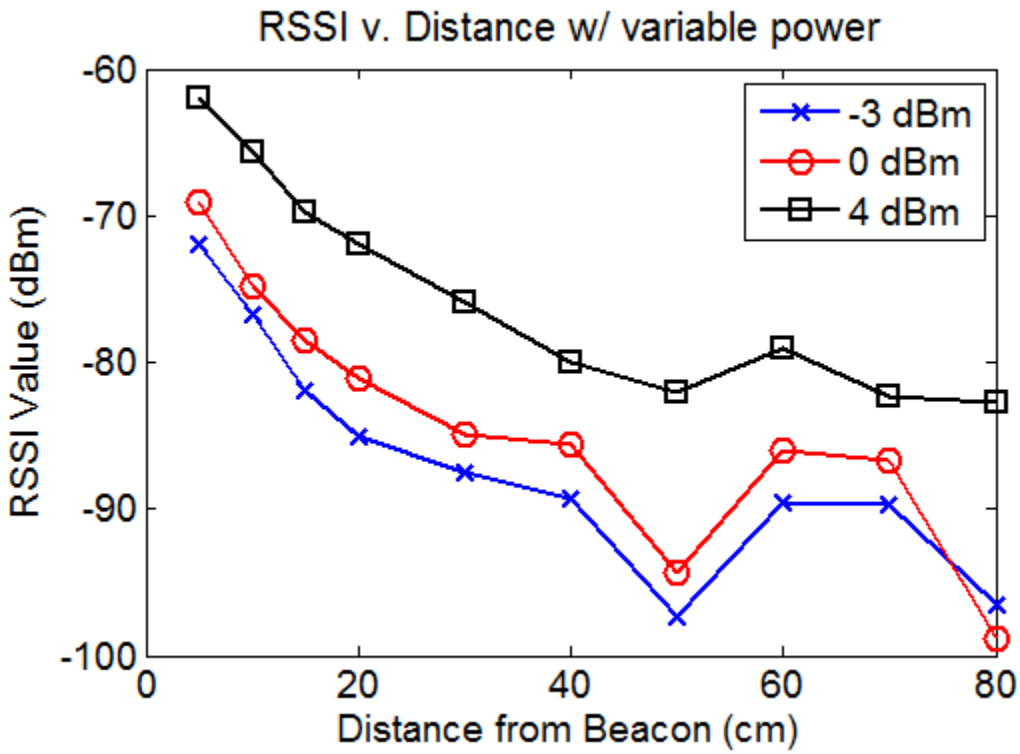

Figure 5.38: RSSI versus distance with different transmit powers

Finally, the influence of platform orientation on the consistency of RSSI values was investigated. Since the ultimate goal of this evaluation was to determine the suitability of RSSI sensing for control algorithms, and since such algorithms involve rotation of the platform, comparing the RSSI values between different rotational angles of the robot was necessary.

The same experiment was performed with the addition of four manual 90° rotations of the platform at each distance. As seen in Figure 5.39, the RSSI is still monotonically decreasing with distance over approximately 50 cm. While there is some variation between orientations, this variation is relatively small – only 5 dBm.

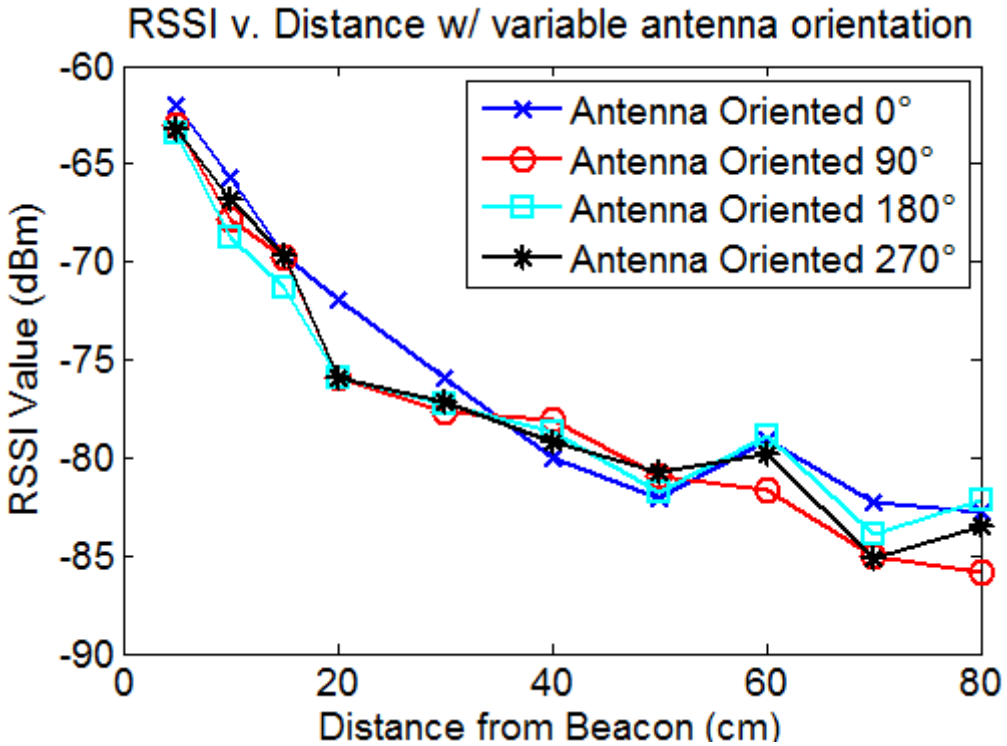

Figure 5.39: RSSI versus distance with different orientations

5.1.3 Summary

The final settings for the radio used the 2425 MHz frequency and 4 dbm transmission power. A quadratic function was used to provide an approximation of distance based on the data from RSSI versus Distance in Figure 5.39. The quadratic equation is shown in **Figure 5.40**, along with the data that was used to derive the equation.

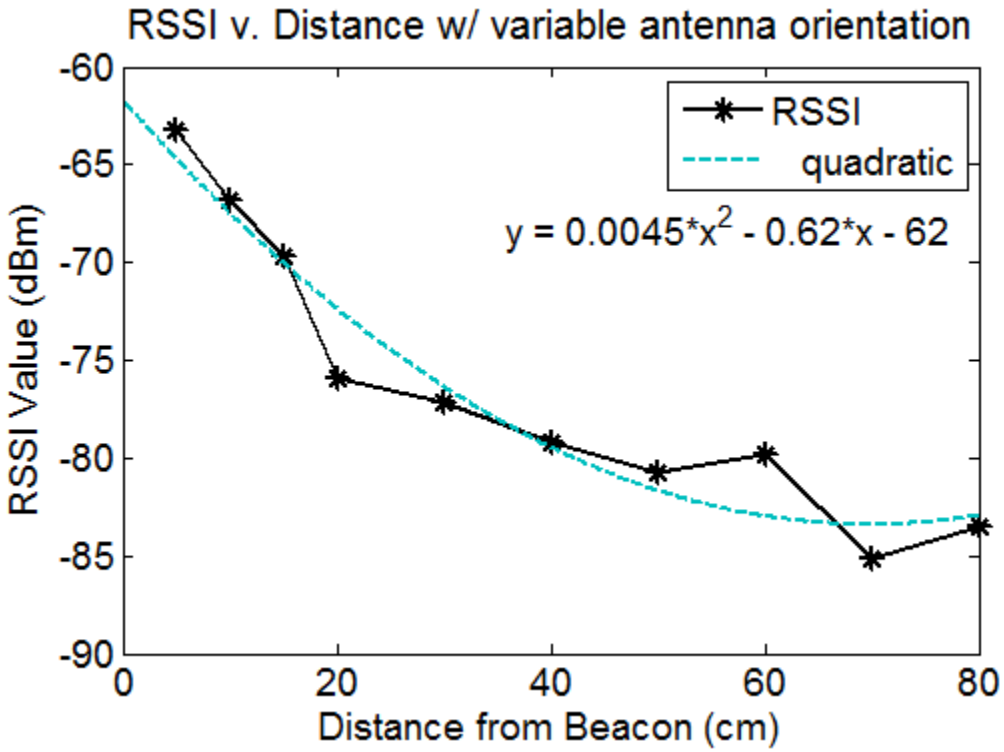

Figure 5.40: Quadratic equation relating RSSI to distance

While RSSI does not provide a great metric for distance between robots over long distances, this data has shown that RSSI is a reasonable distance indicator up to approximately 50 cm. Given that this is approximately 50x the size of the TinyTeRPs, RSSI is a sufficient distance sensor for this platform. Most importantly, RSSI

demonstrates a consistent downward trend versus distance which will make it highly appropriate for the control algorithms described in Chapter 6.

5.3 Optical Mouse Odometry

The use of an optical mouse sensor for odometry is not a new technique [49], [50]. The basic principle is to use the same sensor that a computer uses to track a users hand motion but instead to track a robot. The sensor contains a LED, low resolution camera, and a processing unit. The sensor uses the built in processing unit to process low resolution images, ~16 pixels, to determine direction and magnitude of motion. The advantage of using this sensor for navigation over other sensors, such as IMUs, is the mouse sensor will not suffer from integration error because distance is measured directly. A disadvantage is that the mouse sensor cannot measure rotation, which can cause errors in navigation. A manufacturer of optical mouse sensors pointed out that accuracy of the computer curser is partially based on feedback that the user has and the ability to keep adjusting the mouse.

Even with those challenges, the optical mouse sensor for navigation still seemed worth pursuing. It was quickly found that most mouse sensors were larger than 1.0 cm^2, needed to be within 0.1 cm of the ground, and automatically went into a low power mode and without a way to prevent this from happening. Entering low power mode is a problem because only motion can cause the sensor to return to active mode and a delay caused motion to not be measured while the sensor was actually in motion.

5.3.2 Test Set-up

The smallest sensor found was an ADNK-3530 mouse sensor that included a lens [51–53]. This sensor was chosen to test for a possible module for TinyTeRP. A computer controlled test mechanism, shown in Figure 5.41, was built to test the accuracy and reliability of the optical sensor. The set-up consisted of an old scanner, TI launch-pad, Arduino, and stepper motor board. The TI launchpad, shown in Figure 5.42, was chosen because it was inexpensive, $5.00, and had an usb connection to a computer with pin outs for serial connection to external devices. The Arduino, Figure 5.43, was chosen as it had USB to a computer, easy to program, and 5.0 volt outputs to the stepper board.

The scanner was disassembled to leave only the stepper motor, slide mechanism, and belt. The optical sensor was fitted, with lens, onto the slide mechanism. An Arduino was connected to a stepper motor board. The stepper motor board contained dual H-bridges that allowed more current to the stepper motor than the Arduino's processor could source. The TI launch-pad was connected to the optical sensor and collected the data that the optical sensor measured.

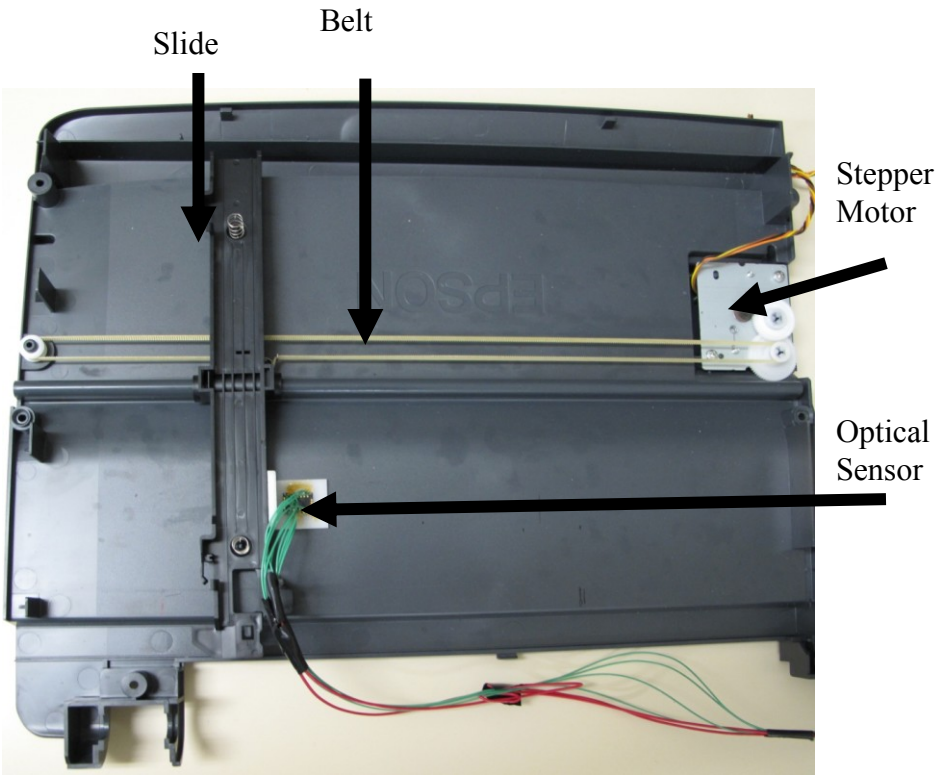

Figure 5.41: Optical mouse sensor test set-up

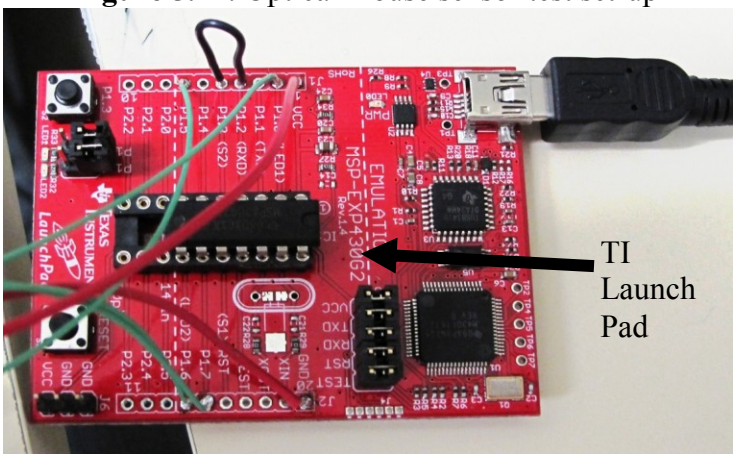

Figure 5.42: Ti launch pad for sensor communication

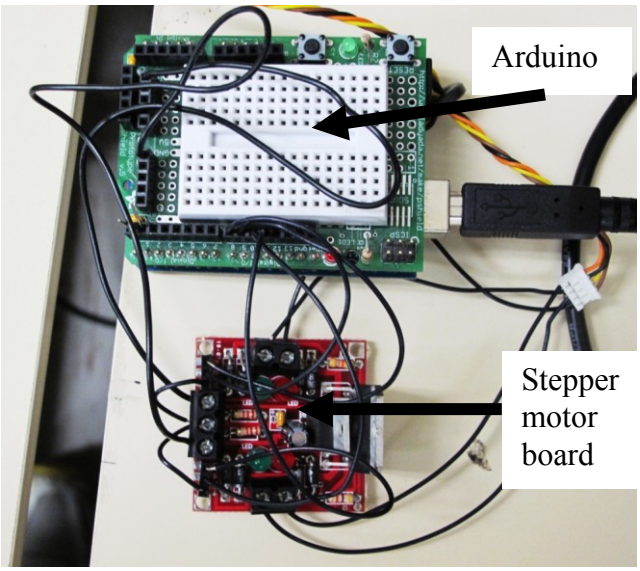

Figure 5.43: Arduino and stepper motor board for stepper motor control

5.3.2 Results

The first experiment performed tested whether the stepper motor and control could repeatedly and precisely move the slide a certain distance. A mark was placed where the slide would begin and then stepper motor was rotated 500 steps, about 8.4 cm. This was several times to see if the slide would repeatedly travel 8.4 cm. It was found that the slide did in fact move 8.4 each time. Thus, it was assumed that if the optical sensor was attached it could move a known distance at a constant rate.

A computer was then connected to both the TI launch-pad and the Arduino to control the movement of the slide and data collection from the optical sensor. This recorded the number of motor steps and the distance that the sensor measured into a file synchronously allowing many trials could be tested without user intervention.

Preliminary results have been obtained, shown in Figure 5.44 and Figure 5.45. Figure 5.44 is the sensor data for the 500 step test. The distance measured should be

8.4 cm. It was found that the actual distance measured was 8.4 cm with a standard deviation of 0.2 cm. Figure 5.45 the data from a 1000 step test. The measured value should be 16.8 cm. The average measured value was 17.4 cm with a standard deviation of 0.1 cm.

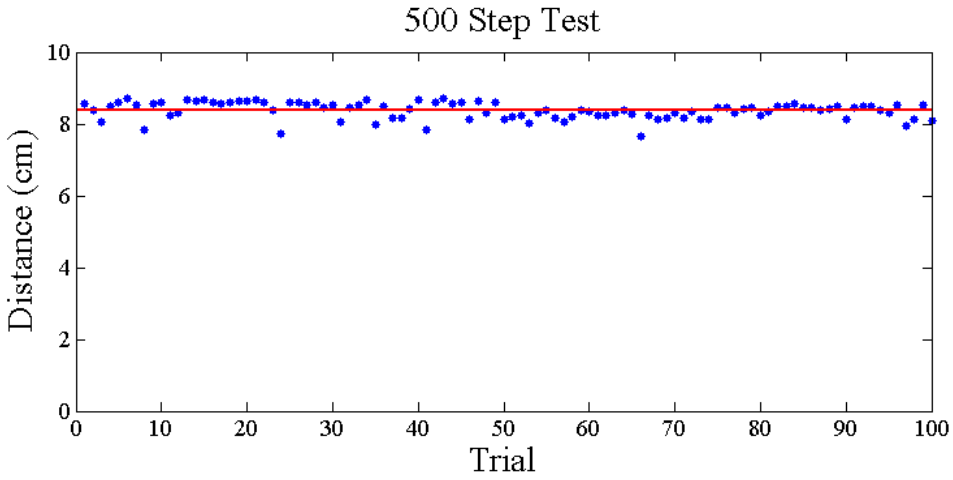

Figure 5.44: Distance traveled versus trial number for 500 step test

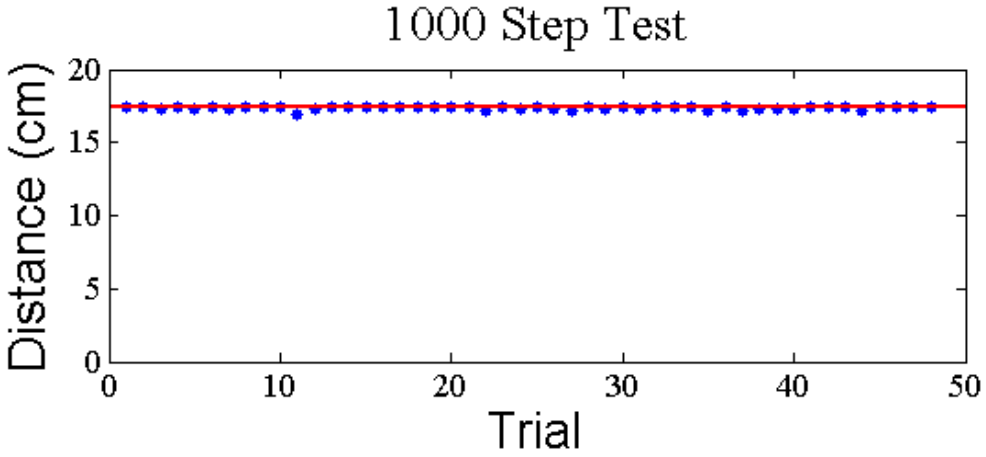

Figure 5.45: Distance traveled versus trial number for 1000 step test

5.3.3 Discussion

Overall it seemed that the sensor maybe useful as a distance measurement device. While this was only meant to be a one degree of freedom (DOF)

test, the results seem promising. An IMU may be added to overcome the inability of the mouse sensor to measure rotation.

Due to using a one DOF test, other challenges could still arise. There could be different accuracy based on direction of motion and surfaces that the sensor is used on. Additionally, speed could be a variable for the performance of the sensors, and this set-up only tested one speed. It is also a rather large sensor, 1.3 x 1.0 cm, which may make this sensor too large for TinyTeRP.

5.2 IMU

5.2.1 Inertial Naviagtion

Intertial navigation is a type of navigation that uses measurements of acceleration and rotation rate to determine position. This method uses inertial measurement units (IMUs) to measure acceleration using accelerometers and the rate of rotation with gyroscopes.

There are inherent drawbacks of using IMUs for navigation because position is never actually measured; rather it is derived from the measurements. For the accelerometers the measurements have to be integrated twice to find linear position. The gyroscopes need to be integrated once to find angular rotation. Integration is known to induce error by compounding small errors continuously. Drift is another error that occurs within IMUs. The measurements tend to "drift" from a value due changes within the sensors. Such changes can include degradation of the sensor, poor calibration, temperature, etc. The error is the compounded with the integration and small errors can turn results quickly into useless information.

The benefit of using inertial navigation is the device is small, lightweight, makes measurements based internal stimuli and can be used in other ways besides navigation. IMUs could be used to determine free fall, object detection, stationary orientation, etc.

5.2.1 IMU navigation Module

An IMU module was chosen as a module to be built for TinyTeRP due to size, cost, and functionality. A COTs six axis accelerometer and gyroscope are available from Invensense. The six axis IMU, the IMU-6000, has a digital output, three axis accelerometer, and three axis gyroscope for $15.00. The IMU-6000 has a small footprint, 0.4 x 0.4 cm.

5.2.2 IMU Module Design

A PCB was created to connect the IMU to the TinyTeRP base module. An IMU-6000 along with a MSP430f2370. The MSP430f2370 communicates to the IMU-6000 through SPI because SPI can handle faster data transfer speeds that I^2C. The MSP430f2370 communicates to the base module through the header with I^2C. This microcontroller was included on the board to process the IMU data. To reduce integration error, sample rates must be high causing the processing speed of the processor to be fast. Integration requires multiplication and addition. Multiplication can take hundreds of processor cycles to complete. The MSP430f2370 includes a hardware multiple, a device that is capable of multiplying numbers in a few processor cycles, which the CC2533 does not have.

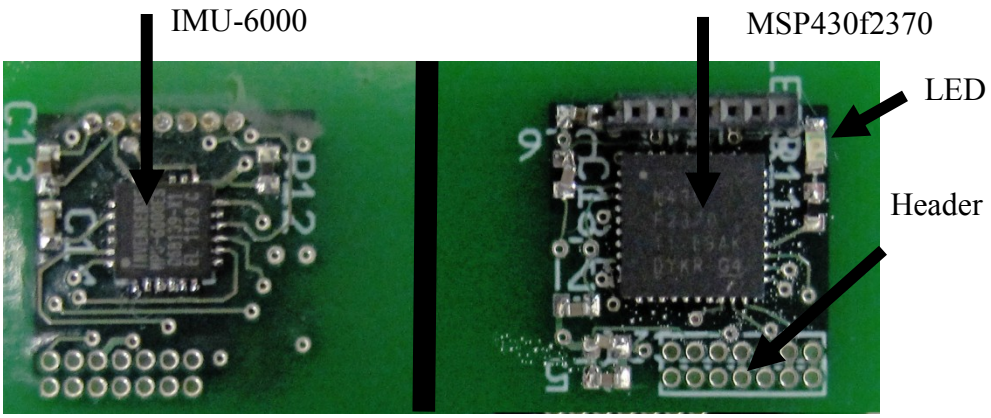

Figure 46: IMU sensor module

5.2.4 Future work

Due to time constraints the IMU module it was never tested. The PCB was ordered and populated. The MSP430f2370 was programmed, successfully, to blink the LED. There still needs to be a program coded to retrieve and process the IMU data.

Chapter 6 Control Logic

6.1 RSSI Navigation

Given the limited computation and sensing resources on TinyTeRP, significant emphasis was placed on designing control algorithms that could demonstrate interesting robot behavior despite these constraints. For example, RSSI only provides an approximation of distance from other robots and does not provide orientation. In addition, as shown in section 5.1.3, the relationship between RSSI and distance is not linear and there is some difference between RSSI at different robot orientations. Rate of packet transmission will also affect the robot's ability to provide a good estimate of RSSI while it is in motion.

A second consideration is the precision of the locomotion module. The base module does not include an on-board voltage regulator which means that voltage applied to the motors changes significantly over the robot's lifespan. While the delrin chassis provides some consistency in robot assembly, the motor placement was not always repeatable, so the same signal applied to both motors resulted in a curved robot trajectory instead of a straight line.

Two algorithms are described below. Both utilize a single transmitting "beacon" that the robots attempt to approach or stay near. In the first algorithm, the robots use previous RSSI measurements along with current RSSI measurements to find a gradient (*Gradient Descent*). The robots then descend this gradient to find the beacon. In the second algorithm, the robots only use current RSSI measurements to stay within a given radius of the beacon (*Vicinity*). This algorithm is especially

interesting because it does not require the robot to have any memory of where it has been.

6.2 Gradient Descent

The first algorithm uses a gradient descent approach to find the transmitting beacon. Only a few constraints were hard coded onto the robot: the robot needed to know when it was close enough to the beacon to stop, when it was too far away to rely on RSSI, and when it was moving toward the beacon. Robot speed was hard coded to match the beacon's packet transmission rate, and the robot ignored any RSSI values received while turning to avoid confusion based on the orientation dependence of RSSI. The basic algorithm is described by the following pseudocode:

```
While (true)
Wait for RSSI packet
Average N RSSI values
Gradient = CurrentAverage – PreviousAverage
If close to the beacon
  STOP
Else if too far away
  STOP
Else if Gradient > 0 (moving away from beacon)
  TURN for fixed time
Else
  Go FORWARD
```

This algorithm was tested on single robots moving toward a beacon (shown in Figure 5.47) and on multiple robots moving toward the beacon. In general, the algorithm was fairly robust and the robot was able to find the beacon most of the time. A packet sniffer was used to record RSSI values during the test and inconsistent RSSI values were generally the cause of test failures. For example, the robot would

record an RSSI value classifying it as “too far away” even though it was close to the beacon. These failure cases are still being investigated.

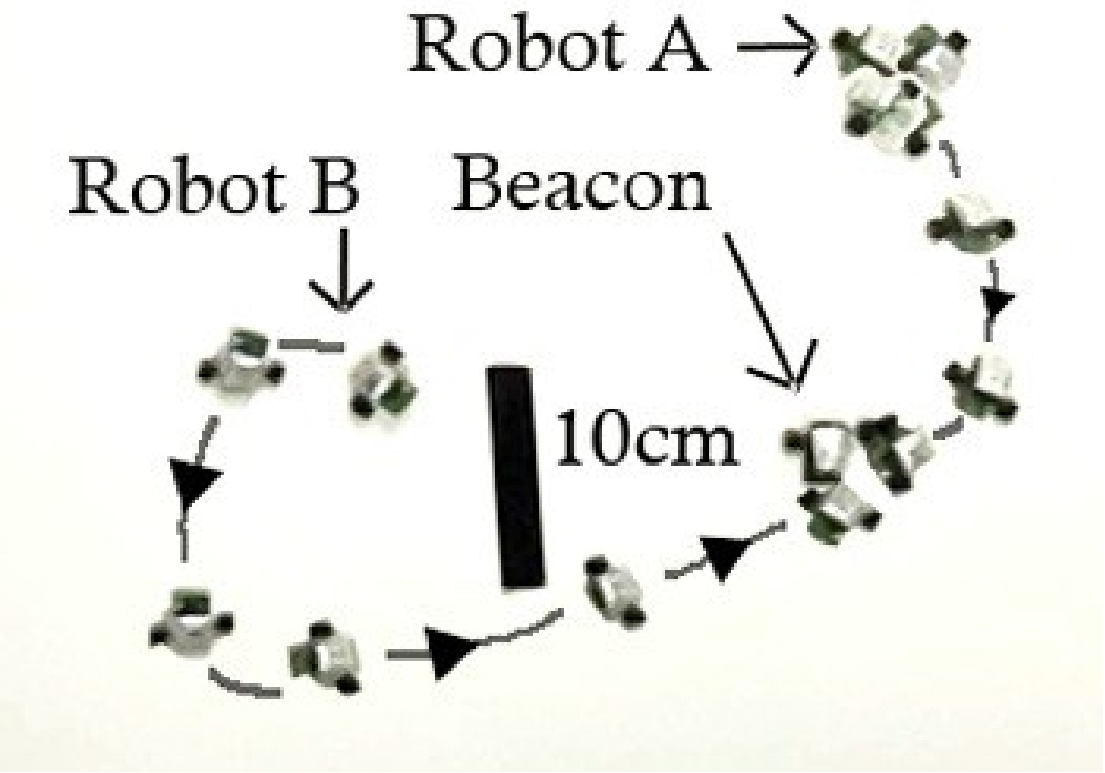

Figure 5.47: Time-lapse of TinyTeRP using gradient descent logic

6.3 Vicinity

A second algorithm was created through collaboration with Dr. Martins. The second algorithm did not calculate a gradient and only used current RSSI values to stay within a defined distance of the transmitting beacon based on a hard coded RSSI threshold. This algorithm requires even fewer computational resources than Gradient Descent since it does not require any memory of a previous state, and as a result, the robot never knows if it is moving closer to the beacon or further away. A hardcoded

variable is used to define the RSSI threshold or radius through which the TinyTeRP travels. A greater threshold means that the TinyTeRP will travel further away from the beacon while a closer threshold will constrain the TinyTeRP to a smaller circle around the beacon. It is important to note that the robot's speed is proportional to its distance away from the beacon. Therefore, it should stay close to the beacon for a longer period of time. The turn behavior is defined by a turn followed by a short forward motion to bring the robot back within the threshold. Algorithms such as this may become especially important as robots are further reducing in size. The basic algorithm is described by the following pseudocode:

```
While (true)
Wait for RSSI packet
If robot is near threshold
  TURN for a fixed time
Else
  Go FORWARD with speed distance from beacon
```

Timelapse of a trial generated path by this algorithm is shown in Figure 5.48. While there is still a great deal to explore using this algorithm, the figure clearly shows that the robot stays within a defined boundary during its wandering over a 25 second time period. The robot actually moved within this region for 2 minutes and failed when it moved too far from the beacon and turns did not bring it back in range. The turn behavior is currently being adjusted to prevent this failure.

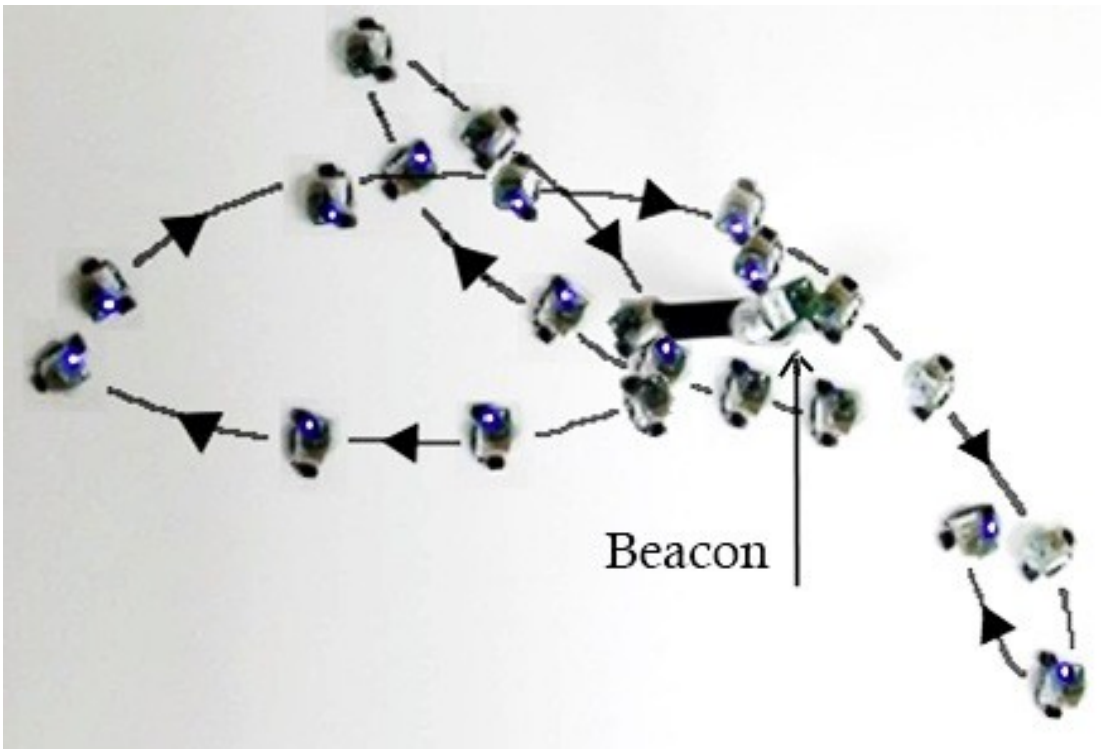

Figure 5.48: Time-Lapse of TinyTeRP using memory less logic

Chapter 7 Conclusion

This work presented the design of an 8.0 cm^3 autonomous mobile robot platform called Tiny Terrestrial Robotic Platform, TinyTerp , shown in Figure 6.49. TinyTeRP has an 802.15.4 wireless radio capable of RF communication that has the ability to transmit data several meters combined with the ability to navigate/localize. A robot with the functionality, low cost ($51.50), speed, and long range communication is not found on another robot of the same size. The final costs for each portion of TinyTeRP are displayed in Table 6.7. TinyTeRP is able to move at speed over ten body lengths per second for several minutes. Several sensing and navigation methods and modules were discussed that show promise for future use on TinyTeRP. Locomotion methods were also discussed with focus on DC motors with wheels as the primary method of locomotion for TinyTeRP. A new thermal actuated leg manufacturing technique is currently being tested and prepared so that polymer legs can be an additional locomotion module for TinyTeRP.

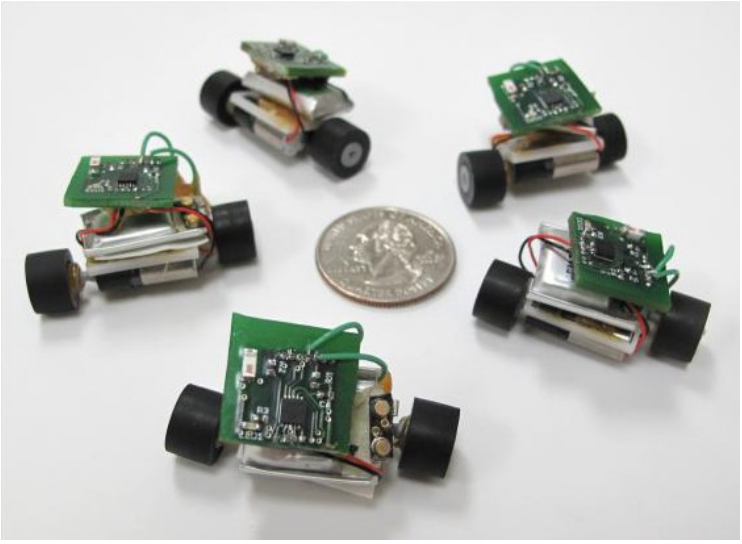

Figure 6.49: Five TinyTeRPs around a quarter

Table 6.7: List of costs for TinyTeRP

Part	Quantity	Cost (10pcs)	Total
Base module PCB	1	$1.10	$1.10
Base module parts	1	$18.30	$18.30
6mm 25:1 geared DC motors	2	$12.00	$24.00
9mm wheels	2	$1.00	$2.00
50 mAh battery	1	$6.00	$6.00
Laser cut chassis	1	$0.10	$0.10
TinyTeRP			**$51.50**

7.1 Future Work

The future of TinyTeRP can be in various directions. TinyTeRP is the beginning of an iterative process that will make the robot smaller. With technology constantly changing, microcontrollers becoming smaller, and batteries with higher energy densities made every year, it is only a matter of time before TinyTeRP will become 1.0 cm^3. TinyTeRP, in its current state, can still be useful to researches interest in 1.0 cm^3 to study control algorithms, locomotion methods, and design techniques that can be used to create smaller robots. Additional work on the thermal legs is another promising interest. About half of the cost of TinyTeRP is in the locomotion module. The polymer legs with patterned silver composite have the ability to dramatically reduce the cost and size of the robot by reducing the cost of the locomotion module.

Appendix A

The devices used to support this project may be useful so they are included here. Probably the most frequently used piece of equipment was an oscilloscope, the Tekronix 2014, shown in Figure A.50. It has a bandwidth of 200 Mhz and was used to test I^2C communication, I/O outputs (including PWM), noise in lines, etc. Further information can be found at: http://www.tek.com/products/oscilloscopes/tds2000/

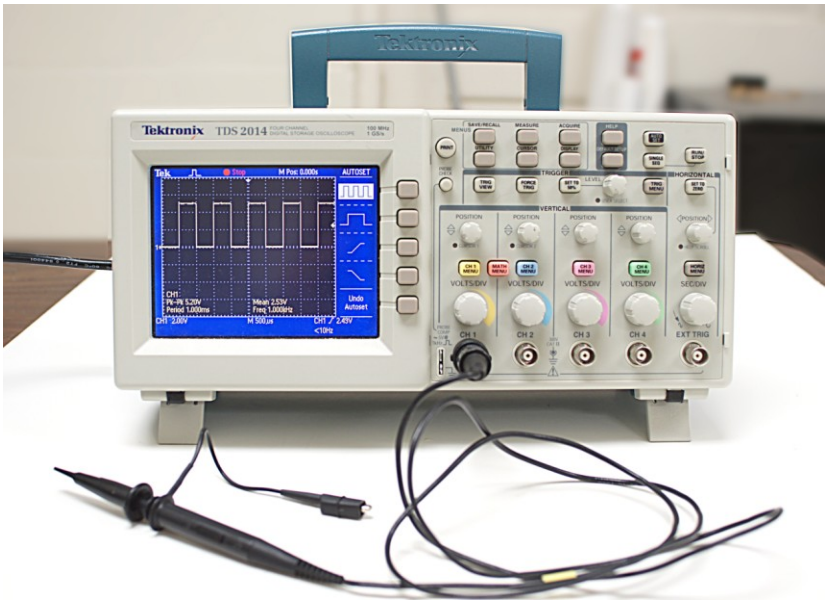

Figure A.50: Tekronix 2014 oscilliscope

Another useful piece of equipment was the "Bus pirate", shown in Figure A.51. This device has the ability to "spy" serial communication, such as the I^2C, and initiate serial communication. The best reason for using this device is it comes assembled and can be assumed to work, allowing the programmer to use interpret serial communication into symbols on a computer. It is available at http://www.sparkfun.com/products/9544 for $30.00. The manual can be found at http://dangerousprototypes.com/docs/Bus_Pirate.

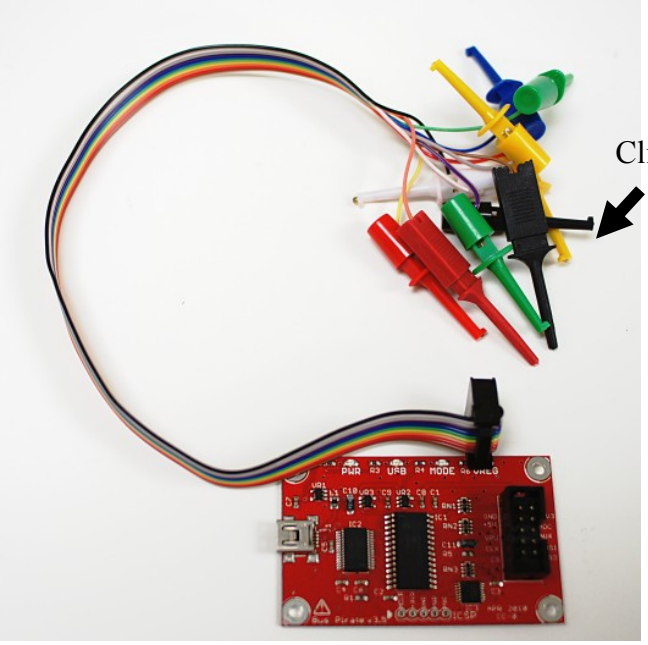

Figure A.51: BusPirate

To use the “bus pirate” in spy mode, connect the clips to the serial communication lines of the device using the serial communication (mosi = data clk = clock). Connect the Bus Pirate to a computer using usb. Thenfollow the following instructions.

1) Install Tera Term
2) Set the com port
3) Type “m” for menu
4) “4” for i2c
5) “(2)” for sniffer

The Figure A**.52** shows the Bus Pirate interface, set-up, and some communication between two devices. The following will help decipher the communication between the two devices:

- “[” = Start bit

- "+" = Space
- "0x1E" = Address with write bit
- "0x06" = Address of register
- "[" = Start bit
- "0x1F" = Address with read bit
- "0x30" = Device response

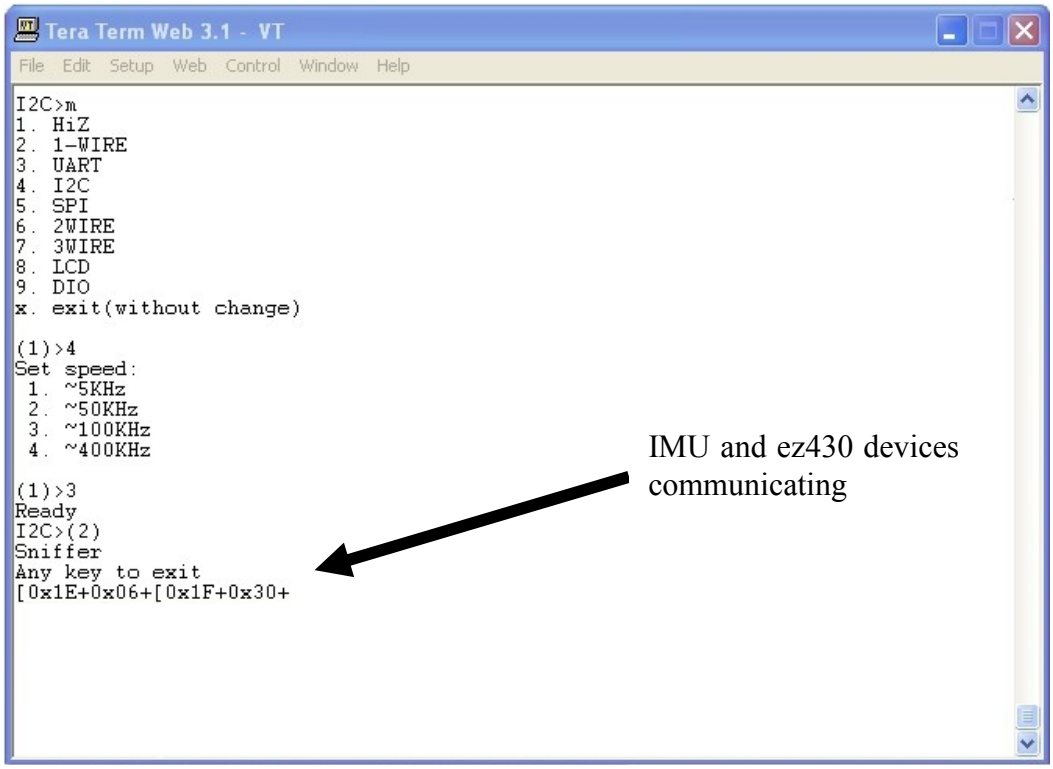

Figure A.52: Spied communication between two devices using I^2C using the bus pirate

Finally a radio packet sniffer, shown in Figure A.53, was used to spy and communicate with the TinyTerp base module [37]. The EZ430 and CC2533 do not have compatible radios so a separate sniffer was purchased. The was assembled be TI and was assumed to work error free. The sniffer served several purposes, capturing radio packets from TinyTeRP, spying between two robots, and sending out commands. Additionally, error rates could be found, various data could be collected, or direct computer to TinyTeRP communication could be used. The sniffer could also

be reprogrammed using the CC debugger, which allowed for different programs to be flashed onto the sniffer board. Over all this was an indispensable device to measure the success of the TinyTeRP base module.

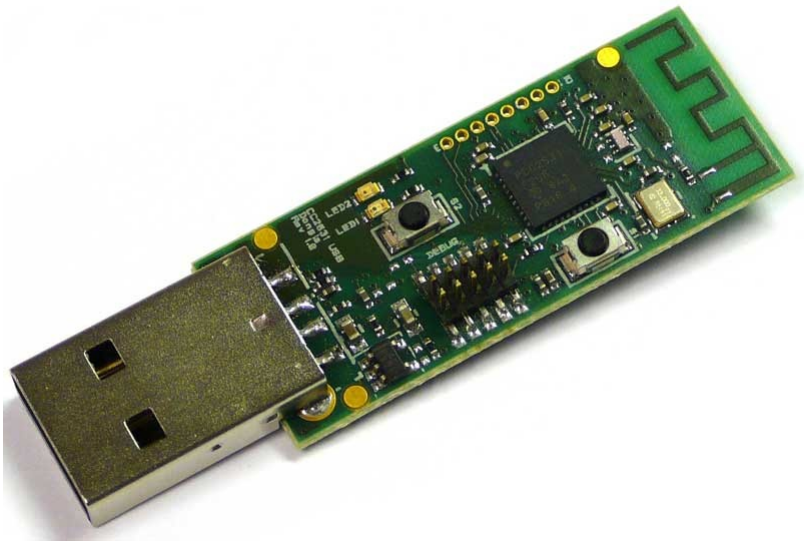

Figure A.53: CC2531 RF sniffer

Bibliography

[1] IRobot, "The iRobot SUGV." [Online]. Available: www.irobot.com/gi/ground/SUGV.

[2] "XM1216 Small Unmanned Ground Vehicle," *Wikipedia*. [Online]. Available: http://en.wikipedia.org/wiki/XM1216_Small_Unmanned_Ground_Vehicle.

[3] G. Caprari and R. Siegwart, "Mobile micro-robots ready to use: Alice," in *2005 IEEE/RSJ International Conference on Intelligent Robots and Systems, 2005. (IROS 2005)*, 2005, pp. 3295- 3300.

[4] G. Caprari, P. Balmer, R. Piguet, and R. Siegwart, "The autonomous micro robot 'Alice': a platform forscientific and commercial applications," in *Proceedings of the 1998 International Symposium on Micromechatronics and Human Science, 1998. MHS '98*, 1998, pp. 231-235.

[5] G. Caprari, K. O. Arras, and R. Siegwart, "The autonomous miniature robot Alice: from prototypes toapplications," in *2000 IEEE/RSJ International Conference on Intelligent Robots and Systems, 2000. (IROS 2000). Proceedings*, 2000, vol. 1, pp. 793-798 vol.1.

[6] A. M. Hoover, E. Steltz, and R. S. Fearing, "RoACH: An autonomous 2.4g crawling hexapod robot," in *IEEE/RSJ International Conference on Intelligent Robots and Systems, 2008. IROS 2008*, 2008, pp. 26-33.

[7] UC Berkeley, "RoACH: A Robotic Autonomous Crawling Hexapod." [Online]. Available: http://robotics.eecs.berkeley.edu/~ronf/Ambulation/Roach.html.

[8] M. Rubenstein, N. Hoff, and R. Nagpal, "Kilobot: A Low Cost Scalable Robot System for Collective Behaviors," Jul. 2011.

[9] A. T. Baisch, C. Heimlich, M. Karpelson, and R. J. Wood, "HAMR3: An autonomous 1.7g ambulatory robot," in *2011 IEEE/RSJ International Conference on Intelligent Robots and Systems (IROS)*, 2011, pp. 5073-5079.

[10] T. Ebefors, J. U. Mattsson, E. Kälvesten, and G. Stemme, "A walking silicon micro-robot," in *Proc. Transducers' 99*, 1999, pp. 1202–1205.

[11] T. Ebefors, E. Kalvesten, and G. Stemme, "Three dimensional silicon triple-hot-wire anemometer based onpolyimide joints," in *, The Eleventh Annual International Workshop on Micro Electro Mechanical Systems, 1998. MEMS 98. Proceedings*, 1998, pp. 93-98.

[12] T. Ebefors, J. U. Mattsson, E. KÃ¤lvesten, and Gã¶. Stemme, "A robust micro conveyer realized by arrayed polyimide joint actuators 1," *Journal of Micromechanics and Microengineering*, vol. 10, pp. 337-349, Sep. 2000.

[13] W. Churaman, "Novel Integrated System Architecture for an Autonomous Jumping Micro-Robot," 2010. [Online]. Available: http://drum.lib.umd.edu/handle/1903/10865.

[14] L. J. Currano and W. A. Churaman, "Energetic Nanoporous Silicon Devices," *Journal of Microelectromechanical Systems*, vol. 18, no. 4, pp. 799-807, Aug. 2009.

[15] W. A. Churaman, A. P. Gerratt, and S. Bergbreiter, "First leaps toward jumping microrobots," in *2011 IEEE/RSJ International Conference on Intelligent Robots and Systems (IROS)*, 2011, pp. 1680-1686.

[16] L. J Currano, W. A. Churaman, J. E. Rajkowski, C. J. Morris, and S. Bergbreiter, "NANOENERGETIC SILICON AS A THRUST ACTUATOR FOR JUMPING MICROROBOTS," in *Solid-State Sensors, Actuators, and Microsystems Workshop*, 2010, pp. 126-129.

[17] N. O. Pérez-Arancibia, K. Y. Ma, K. C. Galloway, J. D. Greenberg, and R. J. Wood, "First controlled vertical flight of a biologically inspired microrobot," *Bioinspiration & Biomimetics*, vol. 6, p. 036009, Sep. 2011.

[18] R. J. Wood, "The First Takeoff of a Biologically Inspired At-Scale Robotic Insect," *IEEE Transactions on Robotics*, vol. 24, no. 2, pp. 341-347, Apr. 2008.

[19] R. J. Wood, S. Avadhanula, R. Sahai, E. Steltz, and R. S. Fearing, "Microrobot Design Using Fiber Reinforced Composites," *Journal of Mechanical Design*, vol. 130, no. 5, pp. 052304-11, May 2008.

[20] C. Perkins et al., "Distance sensing for mini-robots: RSSI vs. TDOA," in *2011 IEEE International Symposium on Circuits and Systems (ISCAS)*, 2011, pp. 1984-1987.

[21] E. Arvelo and N. . Martins, "A Receding Horizon Approach to Systems with Interval-Wise Energy Constraints," presented at the 50th IEEE Conference on Decision and Control, Orlando, Florida, 2011.

[22] W.-J. Ma, E. Arvelo, and N. . Martins, "Designing Networked Control Architectures for Incremental Robustness," presented at the IFAC 18th World Congress, Milano, Italy, 2011.

[23] K. Tossell, A. Hammond, E. Arvelo, and N. C. Martins, "Visual mini-robot identification, tracking and control," MERIT, 2010.

[24] A. P. Gerratt, B. Balakrisnan, I. Penskiy, and S. Bergbreiter, "Batch fabricated bidirectional dielectric elastomer actuators," in *Solid-State Sensors, Actuators and Microsystems Conference (TRANSDUCERS), 2011 16th International*, 2011, pp. 2422-2425.

[25] B. Balakrisnan and E. Smela, “Challenges in the microfabrication of dielectric elastomer actuators,” 2010, p. 76420K-76420K-10.

[26] S. Bergbreiter and K. S. . Pister, “CotsBots: an off-the-shelf platform for distributed robotics,” in *2003 IEEE/RSJ International Conference on Intelligent Robots and Systems, 2003. (IROS 2003). Proceedings*, 2003, vol. 2, pp. 1632-1637 vol.2.

[27] PowerStream, “Batteries and Battery Packs.” [Online]. Available: http://www.powerstream.com/.

[28] T. Watteyne, *eZWSN: Experimenting with Wireless Sensor Networks using the eZ430-RF2500*. [Online]. Available: http://cnx.org/content/col10684/latest/.

[29] Texas Instruments, “MSP430 Wireless Development Tool.” [Online]. Available: http://www.ti.com/tool/ez430-rf2500.

[30] Allegro, “A3901 Dual Full Bridge Low Voltage Motor Driver.” [Online]. Available: http://www.allegromicro.com/en/Products/Part_Numbers/3901/.

[31] Texas Instruments, “CC2533.” [Online]. Available: http://www.ti.com/product/cc2533.

[32] ATMEL, “ATmega128RFA1.” [Online]. Available: http://www.atmel.com/dyn/products/product_card.asp?part_id=4692.

[33] “Antenna Selection Quick Guide.” [Online]. Available: http://www.ti.com/lit/an/swra351/swra351.pdf.

[34] Cadsoft, “Cadsoft EAGLE.” [Online]. Available: http://www.cadsoftusa.com/.

[35] Advanced Circuits, “Full Spec 4-layer Designs $66 each.” [Online]. Available: http://www.4pcb.com/index.php?load=content&page_id=131.

[36] “Debugger and Programmer for RF System-on-Chips,” *Texas Intruments*. [Online]. Available: http://www.ti.com/tool/cc-debugger.

[37] “CC2531 USB Evaluation Module Kit,” *Texas Intruments*. [Online]. Available: http://www.ti.com/tool/cc2531emk.

[38] Case Western Reserve University, “Mini-Whegs Robots.” [Online]. Available: http://biorobots.cwru.edu/projects/whegs/miniwhegs.html.

[39] “Motors and Accessories,” *Solarbotics*. [Online]. Available: www.solarbotics.com.

[40] “Planetary gear motor: GH612,” *Gizmoszone*. [Online]. Available: http://www.gizmoszone.com/.

[41] S. Bergbreiter and K. S. J. Pister, “Design of an autonomous jumping microrobot,” in *Proc. IEEE International Conference on Robotics and Automation (ICRA’07)*, pp. 10–14.

[42] J. E. Rajkowski, A. P. Gerratt, E. W. Schaler, and S. Bergbreiter, “A multi-material milli-robot prototyping process,” in *IEEE/RSJ International Conference on Intelligent Robots and Systems, 2009. IROS 2009*, 2009, pp. 2777-2782.

[43] “DRUM: Rapid Polymer Prototyping for Low Cost and Robust Microrobots.” .

[44] J. Rajkowski, “RAPID POLYMER PROTOTYPINGFOR LOW COST ANDROBUST MICROROBOTS,” University of Maryland, Thesis, 2010.

[45] “PELCO® Conductive Silver 187 (Product # 16045),” *Ted Pella, Inc*. [Online]. Available: www.tedpella.com.

[46] “SYLGARD® 184 SILICONE ELASTOMER KIT,” *Dow Corning*. [Online]. Available: www.dowcorning.com.

[47] J. Hill, R. Szewczyk, A. Woo, S. Hollar, D. Culler, and K. Pister, “System architecture directions for networked sensors,” *ACM SIGPLAN Notices*, vol. 35, no. 11, pp. 93-104, 2000.

[48] G. Blumrosen, B. Hod, T. Anker, D. Dolev, and B. Rubinsky, “Continuous Close-Proximity RSSI-Based Tracking in Wireless Sensor Networks,” in *Wearable and Implantable Body Sensor Networks, International Workshop on*, Los Alamitos, CA, USA, 2010, vol. 0, pp. 234-239.

[49] A. Bonarini, M. Matteucci, and M. Restelli, “Automatic Error Detection and Reduction for an Odometric Sensor based on Two Optical Mice,” in *Proceedings of the 2005 IEEE International Conference on Robotics and Automation, 2005. ICRA 2005*, 2005, pp. 1675- 1680.

[50] Palacin, I. Valganon, and R. Pernia, “The optical mouse for indoor mobile robot odometry measurement,” *Sensors and Actuators A: Physical*, vol. 126, no. 1, pp. 141-147, 2006.

[51] Avagotech, “Sensor Bundle Part Numbers.” [Online]. Available: http://www.avagotech.com/docs/36381.

[52] Avagotech, “ADNK-3530 Sample Kit.” [Online]. Available: http://www.avagotech.com/docs/AV02-1431EN.

[53] Avagotech, “ADNS-3530 Data Sheet.” [Online]. Available: http://www.avagotech.com/docs/AV02-1420EN.